Catecholamine-Induced Lipolysis Inhibits Glucose Uptake and Causes mTOR Complex Dissociation in Adipocytes

Garrett Riley Mullins

Advisor: Thurl Harris, PhD

MS, Biological and Physical Science, University of Virginia, 2013

BA, Molecular Biology, Brigham Young University, 2011

A Dissertation Presented to the Graduate Faculty

of the University of Virginia in Candidacy for the Degree of

Doctor of Philosophy

Department of Pharmacology

University of Virginia

May, 2015

ABSTRACT

Acute hyperglycemia often develops after trauma or major surgery. This condition, termed stress-induced hyperglycemia, contributes to morbidity and mortality and delays patient healing in the ICU. It is a result of systemic insulin resistance caused by the adaptive stress response. Although it directly impacts patient health and has been observed for decades, the pathophysiology of stress-induced hyperglycemia is largely unknown.

Interestingly, β-adrenergic stimulation by catecholamines results in decreased insulin-stimulated glucose uptake in adipocytes. Although this decrease in glucose uptake likely contributes to stress-induced hyperglycemia, the underlying molecular mechanism has not been defined. The work herein has built on the prior literature by examining how β-adrenergic stimulation by catecholamines leads to inhibited insulin action in adipocytes. We provide evidence that β-adrenergic-mediated inhibition of glucose uptake requires lipolysis. We show that lipolysis suppresses glucose uptake by inhibiting the mammalian Target of Rapamycin (mTOR) complexes 1 and 2. In addition, our work shows the mechanism of mTOR inhibition is through the generation of lipid intermediates, likely oxidized neutral lipids, which directly cause mTOR complex dissociation. This work defines a previously unrecognized intracellular signaling pathway whereby lipids generated from lipolysis block insulin signaling, resulting in decreased glucose uptake. This novel mechanism of mTOR regulation likely contributes to the development of stress-induced hyperglycemia and may also play a role in obesity-induced insulin resistance.

ACKNOWLEDGMENTS

I would like to thank my mentor, Thurl E. Harris. I have long said that Dr. Harris is more than a scientific mentor; he is more of a life mentor. His kindness, guidance, and support made it possible for me to be a successful student. Thurl has supported me in picking a project, publishing papers, attending conferences, writing grants, giving presentations, qualifying to become a doctoral candidate, and as my wife and I had two children. He has helped when making the simplest decisions, and the complex. His good natured drive to publish impactful research is contagious, and I would not have accomplished this body of work without his unequivocal support.

I would like to thank my thesis committee. Your insight during and between committee meetings was most helpful. My committee was always willing to help, and ensured that I focus on the important questions. They were essential in taking the right approach, particularly in revising my recent publication.

I would like to thank the members of the Harris lab for being a fun group of lab mates and great collaborators. Specifically, thank you to James, Vidisha, Samantha, Becki, and Salome for performing helpful experiments. Additionally, thank you to Kelley for proofing documents. Outside of Harris lab, I would like to thank Jose Tomsig for his help and expertise in mass spectrometry.

Additionally, I would like to thank the Pharmacology Department. Paula Barrett and Jolene Kidd were instrumental to my success.

Last but not least, I would like to thank my family and friends for their support throughout this process. Specifically, thank you to my wonderful wife, Katie. Without your love and support, I would not be where I am today. I am the luckiest. Also thanks to my father, Dr. Richard E. Mullins, for advice along the way.

TABLE OF CONTENTS

APPENDIX OF FIGURES

CHAPTER 1

CHAPTER 2

CHAPTER 3

CHAPTER 4

CHAPTER 5

APPENDIX OF ACRONYMS

MAG	Monoacylglyceride
DAG	Diacylglycerol
TAG	Triacylglycerol
AC	Adenylyl Cyclase
cAMP	Cyclic Adenosine Monophosphate
ATGL	Adipose Triacylglycerol Lipase
HSL	Hormone-Sensitive Lipase
MGL	Monoacylglycerol Lipase
CGI-58	Comparative Gene Identification-58
PKA	Protein Kinase A
WAT	White Adipose Tissue
ATP	Adenosine Triphosphate
GTP	Guanosine Triphosphate
PDE	Phosphodiesterase
PDE3B	Phosphodiesterase 3B
IRS	Insulin Receptor Substrate
PTB	Phosphotyrosine-Binding
SH2	Src Homology 2
PI3K	Phosphoinositide 3-Kinase
PIP2	Phosphatidylinositol-4,5-Bisphosphate
PIP3	Phosphatidylinositol-3,4,5-Trisphosphate
PDK1	Phosphoinositide-Dependent Kinase-1
GSK3	Glycogen Synthase Kinase-3
FOXO1	Forkhead Box O1
GLUT4	Glucose Transporter Type 4
ICU	Intensive Care Unit

SICU	Surgical Intensive Care Unit
PIKK	PI3K-Related Kinases
mTOR	Mammalian Target of Rapamycin
mTORC1	mTOR Complex 1
mTORC2	mTOR Complex 2
mLST8	Mammalian Lethal with Sec13 Protein 8
PRAS40	Proline-Rich Akt Substrate 40kDa
mSin1	Mammalian Stress-Activated Protein Kinase Interacting Protein
S6K	S6 kinase 1
4E-BP1	4E-Binding Protein 1
AS160	Akt Substrate 160
TSC	Tuberous Sclerosis Complex
GAP	GTPase activating protein
AMPK	5'AMP-Activated Protein Kinase
PA	Phosphatidic Acid
FKBP12	FK506/Rapamycin Binding Protein
FRB	FKBP12-rapamycin-binding
PKC	Protein Kinase C
PH	Pleckstrin Homology
PLD	Phospholipase-D
β-AR	Beta-Adrenergic Receptor
PPAR	Peroxisome Proliferator-Activated Receptor
PTEN	Phosphatase and Tensin Homolog
WT	Wild type
ROS	Reactive Oxygen Species
PUFA	Polyunsaturated Fatty Acid
LOXs	lipoxygenases

TBH	Tert-Butyl Hydroperoxide
BHT	Butylated Hydroxytoluene
BSA	Bovine Serum Albumin
Tw-20	Tween-20
Tx-100	Triton X-100
E600	Diethyl-p-Nitrophenylphosphate
DMEM	Dulbecco's Modified Eagle's Medium
DTT	Dithiothreitol
IBMX	3-Isobutyl-1-Methylxanthine
DMSO	Dimethyl sulfoxide
FBS	Fetal bovine serum
ADA	Adenosine Deaminase
HPLC	High-Performance Liquid Chromatography
LC-MS	Liquid Chromatography-Mass Spectrometry
cps	Counts per Second
SEM	Standard Error of the Mean

CHAPTER 1

GENERAL INTRODUCTION

Catecholaminergic Inhibition of Adipocyte Glucose Uptake

The first law of thermodynamics, often referred to as the law of conservation, states that energy can neither be created nor destroyed. However, energy can be converted from one form into another. Energy homeostasis within a biological system adheres to these principles and is essential to prevent energy wasting by futile cycling. Homeostasis is achieved by crosstalk between opposing signaling pathways; for example, activating catabolic processes in adipocytes will trigger the inhibition of the opposing anabolic signaling. In this way, energy use and storage are carefully controlled on the cellular level, resulting in whole body energy homeostasis. The role of adipose tissue in this balance is vital, and the observed prevalence of metabolic disorders over recent decades has led to increased scientific and clinical interest in how adipose tissue is contributing to these disorders.

When nutrients are plentiful, insulin is released by the pancreas and stimulates anabolic processes such as the absorption of glucose and fatty acids into adipocytes. These substrates are packaged and stored as triacylglyceride (TAG) in cellular lipid droplets through lipogenesis or fatty acid esterification. Stored lipids can then be released when energy is scarce, during periods of fasting or stress, through the action of catecholamines and other factors. These hormones are released in response to the sympathetic nervous system and stimulate lipolysis. Catecholamines stimulate catabolic processes through activation of the β-adrenergic receptor and subsequent activation of adenylyl cyclase (AC), increased cyclic adenosine monophosphate (cAMP), and

activation of protein kinase A (PKA) **(Figure 1.1)**. PKA activates lipolysis by direct phosphorylation of perilipin, a protein that coats the lipid droplet to prevent lipase access, and hormone-sensitive lipase (HSL)(1), as well as indirect activation of adipose triacylglycerol lipase (ATGL). Perilipin has dual roles in regulating lipolysis; under basal conditions, it protects the lipid droplet from lipase action, whereas in PKA stimulated cells it facilitates lipid hydrolysis (2, 3). ATGL catalyzes the first step in the breakdown of TAG, removing an acyl chain to form diacylglycerol (DAG) (4). Full activation of ATGL requires binding with its co-activator, Comparative Gene Identification-58 (CGI-58). Current data indicate that PKA-mediated phosphorylation of perilipin leads to the release of CGI-58 from perilipin, allowing CGI-58 to interact with ATGL to promote its full activation **(Figure 1.1)** (5). Phosphorylation of HSL by PKA results in a 3-fold increase in HSL catalytic activity and translocation from the cytosol to the lipid droplet (6, 7). HSL is also capable of creating DAG from TAG, but its central role in white adipose tissue (WAT) is to hydrolyze DAG to release a fatty acid and monoacylglyceride (MAG) (8). The last step in lipolysis is performed by monoacylglycerol lipase (MGL), which hydrolyzes MAG to form glycerol and a fatty acid **(Figure 1.1)**. These products of lipolysis are subsequently exported from the adipose tissue into circulation for energy use by other tissues (9) and they may impact adipocyte signaling. However, their potential role as signaling molecules has been underappreciated (10).

Each of these pathways, anabolic and catabolic, have mechanisms to oppose one another to prevent futile cycling and conserve cellular adenosine triphosphate (ATP). Although conserved and considered beneficial, opposition between these pathways can contribute to metabolic disorders, such as insulin resistance, when not properly regulated. The mechanism by which anabolic signaling inhibits catabolic signaling in adipocytes is fairly well defined. Briefly,

insulin leads to the activation of the Akt kinase through direct phosphorylation by insulin signaling cascades (11). Akt acts on many substrates with diverse cellular functions; one of which is the activation of phosphodiesterase 3B (PDE3B), resulting in a higher rate of cAMP degradation (12, 13). The depletion of cAMP as a result of Akt activity inhibits catabolic signaling due to decreased PKA and lipase activity.

The mechanism of crosstalk from catabolic processes to anabolic signaling is largely unknown. It has been established that catecholamines, which activate catabolic signaling, inhibit the anabolic process of insulin-stimulated glucose uptake in adipocytes. This inhibition of glucose uptake was first observed and reported by Green et al. in 1983 **(Figure 1.2)** (14), when our knowledge of the insulin signaling pathway was very limited. Ten years later, Carpene et al. (15) established that the adrenergic inhibition of insulin-stimulated glucose transport was specifically mediated by stimulation of the beta-3 adrenergic receptor in rat adipocytes. Although this inhibition of glucose uptake has been observed by multiple groups over 30 years (14-19), the mechanistic details and potential physiologic implications of this phenomenon have remained unclear. The goal of this work is to describe this molecular mechanism.

Adipocyte Insulin Signaling and Glucose Uptake in Whole-Body Glucose Homeostasis

Proper regulation of insulin-stimulated glucose uptake is essential for human health and survival. Along with the liver, muscle, and brain, adipose tissue is insulin-sensitive and together these tissues' response to insulin tightly regulates systemic blood glucose. Although they each have unique roles, improper function of the insulin signaling pathway in any of these tissues will contribute to the development of metabolic diseases, such as diabetes. The physiological effects

of insulin are generally propagated through reversible protein phosphorylation. The insulin receptor and insulin receptor substrates (IRS) comprise the genesis of the insulin signaling pathway, where insulin binding induces a conformational change resulting in receptor tyrosine auto-phosphorylation (20). These phosphorylated tyrosine residues recruit proteins containing phosphotyrosine-binding (PTB) domains, such as IRS (21). Key tyrosine residues within the IRS are subsequently phosphorylated, which are recognized by the Src Homology 2 (SH2) domain of phosphoinositide 3-Kinase (PI3K), a lipid kinase (22). PI3K then phosphorylates phosphatidylinositol-4,5-bisphosphate (PIP2) to form phosphatidylinositol-3,4,5-trisphosphate (PIP3) and PIP3 recruits proteins containing the pleckstrin homology (PH) domain, such as phosphoinositide-dependent kinase-1 (PDK1), mammalian Target of Rapamycin Complex 2 (mTORC2), and Akt (22, 23). PDK1 directly phosphorylates Akt at threonine 308 (T308), while mTORC2 phosphorylates Akt at serine 473 (S473) to fully activate the Akt kinase **(Figure 1.3)** (24). Once released into the cytosol, Akt mediates most of the metabolic actions of insulin through the phosphorylation of glycogen synthase kinase-3 (GSK3), Akt substrate of 160 kDa (AS160), and forkhead box O1 (FOXO1), and is necessary for glucose uptake, glycogen synthesis, and gluconeogenesis (22).

While whole-body glucose homeostasis depends on the effects of insulin on multiple tissues, insulin resistance in one tissue is often sufficient to cause hyperglycemia. For example, adipocyte-specific GLUT4-/- mice develop systemic insulin resistance and hyperglycemia (25). In addition, mice lacking an essential component of mTORC2, rictor, in adipose tissue alone also develop whole-body insulin resistance and hyperglycemia (26). These findings indicate that insulin resistance or decreased glucose uptake in adipocytes alone can lead to systemic

hyperglycemia, which highlights the importance of insulin action on adipose tissue to maintain whole-body glucose homeostasis.

In addition to improper adipocyte glucose uptake, adipocyte lipolysis has also been implicated in the development of whole-body insulin resistance. Mice lacking either ATGL or MGL have decreased levels of lipolysis and show improved glucose tolerance and are resistant to diet-induced insulin resistance (27, 28). Although our work shows that lipolysis leads to acute insulin resistance in adipocytes, adipocyte glucose uptake only accounts for as little as 10% of total glucose uptake, with skeletal muscle accounting for up to 85% (25). This suggests that while adipocyte lipolysis affects insulin action in adipose tissue, it must also impact other tissues, specifically liver or skeletal muscle, to contribute to hyperglycemia. Hepatic glucose production is inhibited by insulin and is thought to be resistant to insulin-mediated suppression in the development of type 2 diabetes. It has recently been proposed that insulin suppression of hepatic glucose production is through reductions in hepatic acetyl CoA by suppression of lipolysis in white adipose tissue. A decrease in hepatic CoA was shown to reduce pyruvate carboxylase activity and subsequently reduce hepatic glucose production (29). This suggests that an elevation in lipolysis due to insulin resistance in adipose tissue may lead to an increase in hepatic glucose production, which will contribute to whole-body hyperglycemia. Furthermore, lipid release from adipose tissue during lipolysis leads to lipid accumulation in both liver and skeletal muscle, which is thought to inhibit insulin action in these tissues (30-32). Although more work is required to confirm these data and investigate more fully how both insulin resistance and lipolysis in adipose tissue may lead to systemic insulin resistance, these studies are beginning to highlight possible mechanisms, which may significantly contribute to the development of systemic hyperglycemia.

Stress-Induced Hyperglycemia

As previously mentioned, acute hyperglycemia often develops after trauma or major surgery, particularly surgery within the abdominal cavity such as coronary bypass procedures (33). This stress-induced hyperglycemia contributes to mortality and delays healing in post-surgery and ICU patients and is a result of systemic insulin resistance caused by the adaptive stress response (34). The stress response to injury is characterized by rapid activation of the neuroendocrine and inflammatory systems to cause a metabolic state of stress. As a result, anabolic processes are inhibited while catabolic signaling is enhanced to provide substrates for tissue healing (34-36). This is achieved through the release of catabolic agents such as catecholamines, cortisol, glucocorticoids, and inflammatory cytokines (37), leading to the observed stress-induced hyperglycemia. In 1980, Deibert et al. used an insulin clamp in humans to show that epinephrine infusion resulted in hyperglycemia due to decreased glucose metabolism, and that simultaneous propranolol infusion rescued the effects of epinephrine (16). This demonstrated that, similar to catecholamine-mediated inhibition of glucose uptake in adipocytes, epinephrine-mediated hyperglycemia requires beta-adrenergic stimulation.

Until the 1990s, even extreme cases of hyperglycemia after surgery or during critical illness were tolerated without treatment because a high blood glucose concentration was thought to be an evolutionarily conserved response that was beneficial for recovery of the patient (38). This idea was introduced in 1959 by a pioneer of surgical technique, Dr. Francis Daniel Moore. Dr. Moore stated that excess glucose is required to support the energy needs of tissue repair (39), which was generally accepted because the adverse effects of acute hyperglycemia were not known at the time. While it may be that hyperglycemia in response to trauma is actually

beneficial in the absence of modern healthcare, it has been demonstrated that it has negative effects during recovery in the ICU. Since 2001, several clinical trials have shown that insulin therapy to maintain blood glucose at a more normal range decreases morbidity and mortality in critically ill surgical patients (38). This improvement is thought to be attributed to a decrease in infection-related complications and faster wound healing, and as a result, blood glucose monitoring and insulin therapy have become general practice in the ICU. Although it has clear benefits, insulin treatment to reduce hyperglycemia has conflicting evidence regarding the aggressiveness of the insulin treatment (40, 41), and insulin therapy can result in hypoglycemic incidents, leading to increased complications and mortality rates (42).

In 2001 van den Berghe et al. published results from the Leuven Landmark study, where they investigated the benefits of intensive versus conventional insulin therapy in both diabetic and nondiabetic patients during recovery in the surgical ICU. In this study, the fasting blood glucose target range was 80-110 mg/dl for intensive insulin therapy group, and 180-200 mg/dl for conventional insulin therapy group **(Figure 1.4)**. They observed a lower mortality rate, as well as lower frequency of septicemia and other complications in the intensive versus conventional group (41, 43). In the 10 years preceding this study, several clinical trials had observed a correlation between lower blood glucose and improved outcomes as summarized by Butler et al. (38). These observations helped establish the protocol for conventional insulin therapy, but the Leuven Landmark study supported stricter control of blood glucose. In 2009 the NICE-SUGAR (Normoglycemia in Intensive Care Evaluation and Survival Using Glucose Algorithm Regulation) study was meant to test the results of the Leuven Landmark study on a larger scale. Rather than being tightly controlled in one hospital system, the NICE-SUGAR study included hospitals from all around the world, and is the largest study to date of glycemic control

in critically ill patients. This study concluded that intensive insulin therapy has no benefit, and may even increase patient risk, when compared to conventional insulin therapy (40, 43, 44). This finding is likely due to the increased incidence of hypoglycemic shock. As a result of inconsistent methods, the protocols and interpretation of data in the NICE-SUGAR study have been widely criticized (43, 45). In addition, the target range for blood glucose in the control group were lower than the Leuven study, making the NICE-SUGAR trial not a true confirmation of the Leuven study **(Figure 1.4)** (43). Nevertheless, the conflicting results from these studies highlight the benefits of uncovering the molecular mechanisms that contribute to hyperglycemia in the critically ill (35). This knowledge will lay the groundwork for better treatment options to control blood glucose and minimize the risk of hypoglycemia during recovery in the ICU.

Although the stress response affects many tissues and signaling pathways, it has been shown that mice develop adipose tissue insulin resistance very rapidly after surgery and hemorrhage, and impaired insulin action in adipose tissue can result in whole body insulin resistance and hyperglycemia (26, 46, 47). Therefore, the impact of the adaptive stress response on insulin signaling specifically in adipose tissue may contribute to stress-induced hyperglycemia. In adipose tissue, the PKA/cAMP pathway is activated through stimulation of the β-adrenergic receptor, which leads to an acute adipose tissue-specific decrease in insulin-stimulated glucose uptake (14, 15, 19). Furthermore, after heart surgery it is common to infuse norepinephrine to cause an increase in contractility, and catecholamine infusion causes both peripheral insulin resistance and defects in adipocyte insulin signaling (16). This suggests that catecholamine infusion after surgery may be inadvertently contributing to hyperglycemia during patient recovery. While we know that β-adrenergic stimulation dampens insulin-stimulated glucose uptake in adipocytes and inhibition of glucose uptake in adipose tissue alone leads to

systemic hyperglycemia (26), the specific mechanism by which this happens and its possible contribution to stress-induced hyperglycemia are unknown.

mTOR Regulation and Insulin Resistance

Discoveries over the past decade have shown that mammalian Target of Rapamycin (mTOR) integrates nutrient and growth factor signaling to regulate several anabolic processes including cell proliferation, protein translation, insulin-stimulated glucose uptake, and lipid biosynthesis (48, 49). Consequently, mTOR deregulation is prevalent in human diseases such as cancer and type 2 diabetes (50). These observations have led to increased scientific and clinical interest in how mTOR is regulated. mTOR is a serine/threonine protein kinase that interacts with multiple proteins to form at least two distinct complexes: mTOR complex 1 (mTORC1) and mTOR complex 2 (mTORC2). mTOR belongs to the family of PI3K-related kinases (PIKK), and has a C-terminal protein kinase domain that is similar to the lipid kinase PI3K.

mTORC1 contains mTOR, raptor (regulatory associated protein of Tor), mLST8 (mammalian lethal with Sec13 protein 8), PRAS40 (proline-rich Akt substrate 40kDa), and Deptor (DEP-domain-containing mTOR-interacting protein) and integrates input from oxygen, energy status, amino acids, and growth factors to regulate protein translation, autophagy, and anabolic metabolism (51). The best characterized mTORC1 substrates are S6 kinase 1 (S6K) and 4E-binding protein 1 (4E-BP1), each of which regulates protein translation. Raptor regulates mTORC1 assembly and provides the substrate-binding domain to allow for substrate specificity. Because raptor is responsible for recruiting mTORC1 substrate, complex dissociation eliminates the specific kinase activity of mTORC1 (52). Although a central part of the complex, the role of

mLST8 is unknown because its deletion has no apparent effect on mTORC1 activity. PRAS40 and Deptor repress mTORC1 in the dephosphorylated state, but are phosphorylated by mTOR when activated. The phosphorylation of PRAS40 and Deptor weaken their association with the kinase complex, promoting its activity (51). mTORC1 is regulated by many factors, either through direct modification of proteins within the complex, or through regulation of Rheb, a small GTPase that directly interacts with and activates mTORC1 when bound to GTP. The insulin signaling cascade activates mTORC1 through activation of Rheb. On activation by insulin signaling, Akt phosphorylates tuberous sclerosis complex 2 (TSC2), which, as a complex with TSC1, is the GTPase activating protein (GAP) for Rheb. When active, TSC2/TSC1 inhibits mTORC1 activity by facilitating the conversion of Rheb-GTP to Rheb-GDP **(Figure 1.5)**. The phosphorylation of TSC2/TSC1 in response to insulin or other growth factors represses its GAP activity, increasing the presence of Rheb-GTP and mTORC1 action (51). Depletion of energy in the form of oxygen, amino acids, or ATP also inhibits mTORC1. The signaling of low ATP levels to mTORC1 is also mediated by TSC2, and requires 5'AMP-activated protein kinase (AMPK). An increase in the AMP/ATP ratio activates AMPK through direct binding of AMP to AMPK, triggering a conformational change that allows the kinase to become active. AMPK then directly phosphorylates TSC2 in a similar manner to Akt **(Figure 1.5)** (51). AMPK also directly phosphorylates raptor, which is thought to inhibit mTORC1 activity. Another noteworthy mechanism of mTORC1 regulation is by the phospholipid phosphatidic acid (PA). PA has been shown to bind directly to the FKBP12-rapamycin-binding (FRB) domain of mTOR, resulting in mTORC1 activation. This is thought to activate mTORC1 through strengthening the interaction between proteins in the complex (53, 54). Interestingly, chronic activation of mTORC1 has been implicated in the development of insulin resistance through negative feedback inhibition of the

insulin receptor substrate by S6K **(Figure 1.5)** (55). This suggests that mTORC1 activity must be carefully balanced to maintain insulin action.

mTORC2 contains mTOR, rictor (rapamycin insensitive companion of TOR), mSin1 (mammalian stress-activated protein kinase interacting protein), Protor-1 (protein observed with Rictor-1), mLST8, and Deptor and is activated by growth factors through a mechanism that is largely unknown (56). It regulates cell survival and metabolism by phosphorylating Akt, protein kinase C (PKC), and serum and glucocorticoid-inducible kinase (SGK). Unlike in mTORC1, mLST8 is required for mTORC2 activity. Rictor and mSin1 stabilize each other, providing structural integrity to the complex, and mSin1 contains a PH-like domain, suggesting it may be involved in localization of the kinase complex (51). Although less is known about mTORC2 regulation, it is also activated by insulin and other growth factors in a PI3K-dependent manner (57), and phospholipase-D (PLD) dependent accumulation of PA has also been implicated in mTORC2 activity (58, 59). In addition to regulating cell survival, mTORC2 plays an important role in insulin-stimulated glucose uptake. Phosphorylation of Akt at Serine 473 by this kinase complex is necessary for Akt activity on AS160, which is essential for GLUT4 translocation to the plasma membrane (26, 60). AS160 is a Rab GTPase that is inactivated on phosphorylation by Akt. This allows Rab-GTP to facilitate GLUT4 translocation, leading to glucose uptake in response to insulin (61). Like mTORC1, mTORC2 complex integrity is essential for kinase substrate specificity, and complex dissociation renders the kinase complex inactive (62). Importantly, adipocyte-specific rictor knockout mice develop systemic insulin resistance due to decreased AS160 phosphorylation by Akt (26). In addition, lipid accumulation in the liver has been shown to directly inhibit insulin signaling by decreasing mTORC2 complex integrity and activity (63), implicating mTORC2 deregulation in obesity-induced insulin resistance.

mTORC1 is sensitive to acute treatment with rapamycin, which interacts with FKBP12 and binds to the FRB domain of mTOR, while mTORC2 is rapamycin resistant. However, long-term treatment with rapamycin will also inhibit mTORC2 (64, 65), and can lead to impaired insulin signaling and glucose uptake in humans (66-68). In addition, recent studies have suggested that impaired insulin signaling and decreased glucose tolerance during rapamycin treatment is due to inhibition of mTORC2 (26, 68, 69). Together, these findings highlight the possibility of an endogenous mTOR inhibitor contributing to the development of insulin resistance.

Figure 1.1 Activation of Lipolysis by Catecholamines in the Adipocyte.

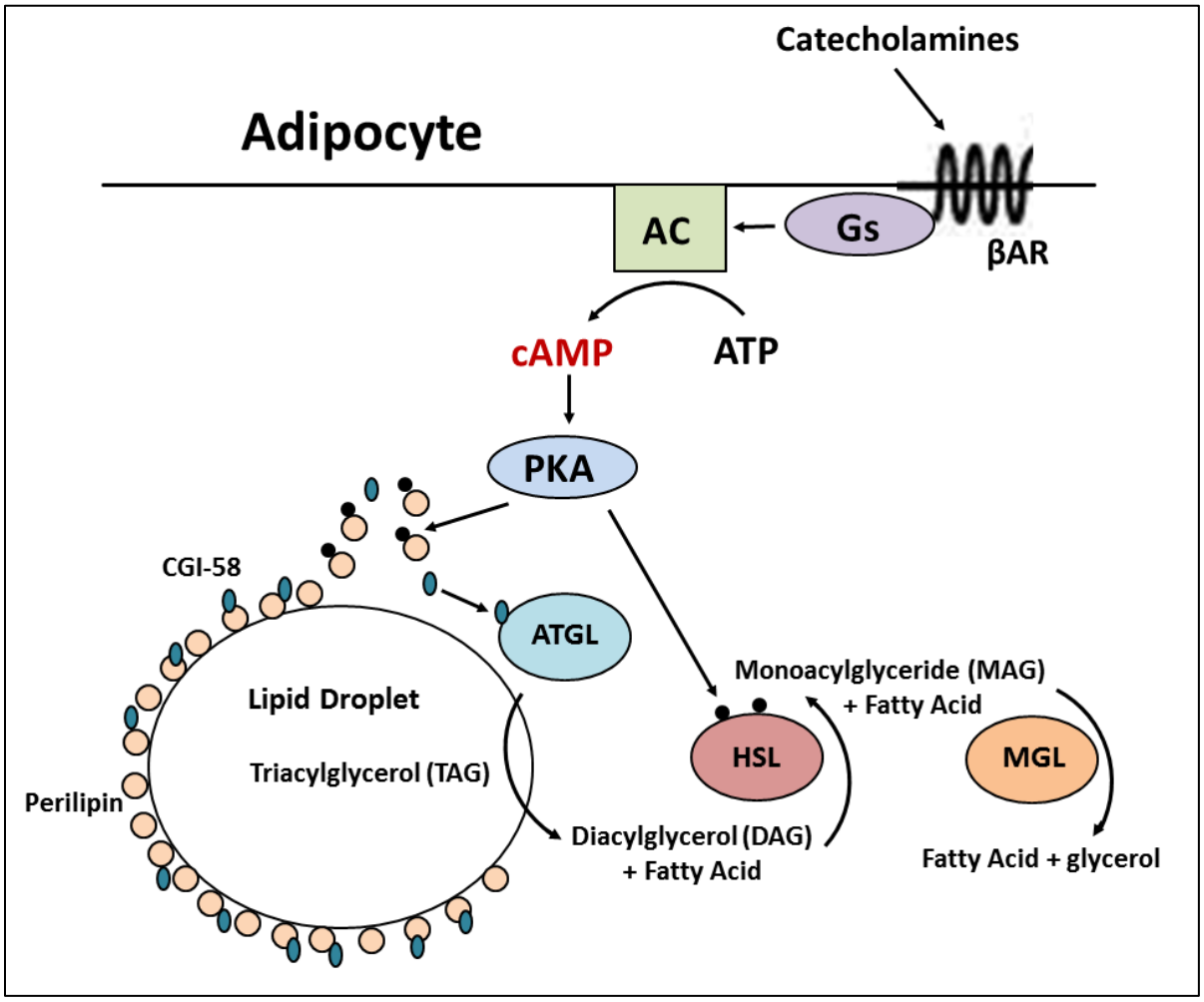

Figure 1.1 Activation of Lipolysis by Catecholamines in the Adipocyte. Catecholamine action on the β-adrenergic receptor leads to increased concentrations of cAMP and activation of PKA. PKA phosphorylates Perilipin and HSL to initiate lipolysis, or the breakdown of stored TAG into lipolytic products DAG, MAG, fatty acids, and glycerol. Perilipin coats the lipid droplet to protect the stored lipids from lipase activity and prevents CGI-58 from activating ATGL, but PKA phosphorylation of perilipin allows it to move off the lipid droplet, letting lipolysis proceed.

Figure 1.2 First Report that Catecholamines Inhibit Glucose Uptake in Adipocytes [Taken from Reference (14)].

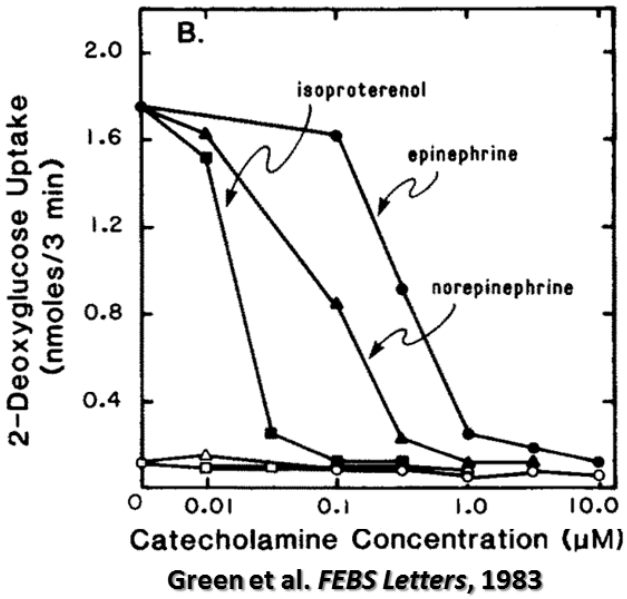

Figure 1.2 First Report that Catecholamines Inhibit Glucose Uptake in Adipocytes [Taken from Reference (14)]. "Adipocytes were incubated at 37°C without (open symbols) or with (closed symbols) insulin (25 ng/ml) plus the indicated concentrations of epinephrine, norepinephrine, or isoproterenol. After 1 h, 2-deoxyglucose uptake was measured… 2-Deoxy-D-[I-^{3}H]-glucose (1.6 mCi/mmol) was added to a final concentration of 0.1 mM. The assays were terminated 3 min later by transferring 200 μl samples of the cell suspension to plastic microtubes containing silicone oil (100 μl). The tubes were centrifuged for 30 sec in a Beckman 'Microfuge', and the assay was considered terminated when centrifugation began. The tubes were cut through the oil layer with a razor blade, and the radioactivity in the cell pellet was measured in a liquid scintillation counter" (14). These data formed the question we address herein: What is the mechanism of this catecholamine-mediated inhibition of glucose uptake?

Figure 1.3 Insulin Signaling Leads to GLUT4 Translocation to the Plasma Membrane.

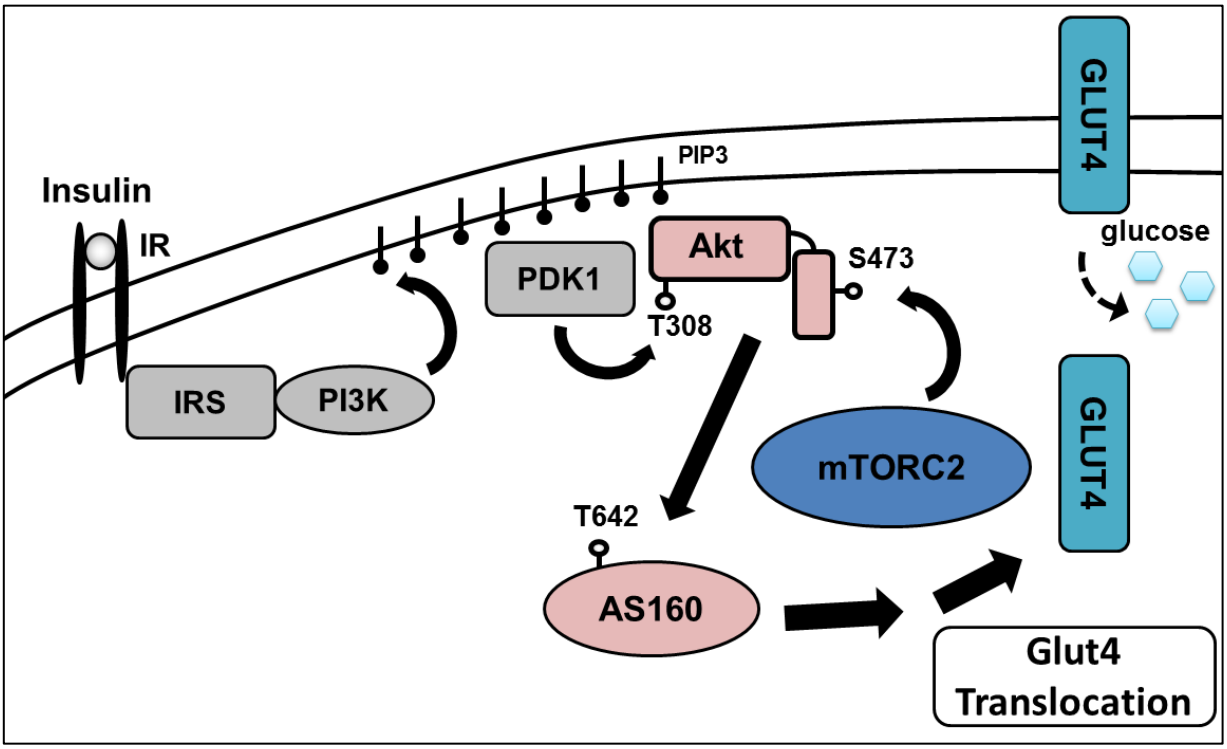

Figure 1.3 Insulin Signaling Leads to GLUT4 Translocation to the Plasma Membrane. Full activation of Akt requires 2 phosphorylation events: Phosphorylation at T308 by PDK1, and phosphorylation at S473 by mTORC2. PDK1 and mTORC2 are activated by insulin, but the detailed mechanism leading to mTORC2 activation is largely unknown. When fully active, Akt phosphorylates AS160, which leads to GLUT4 translocation to the plasma membrane and subsequent glucose uptake in response to insulin.

Figure 1.4 Comparison of the Leuven Landmark Study and the NICE-SUGAR Study [Taken from Reference (43)].

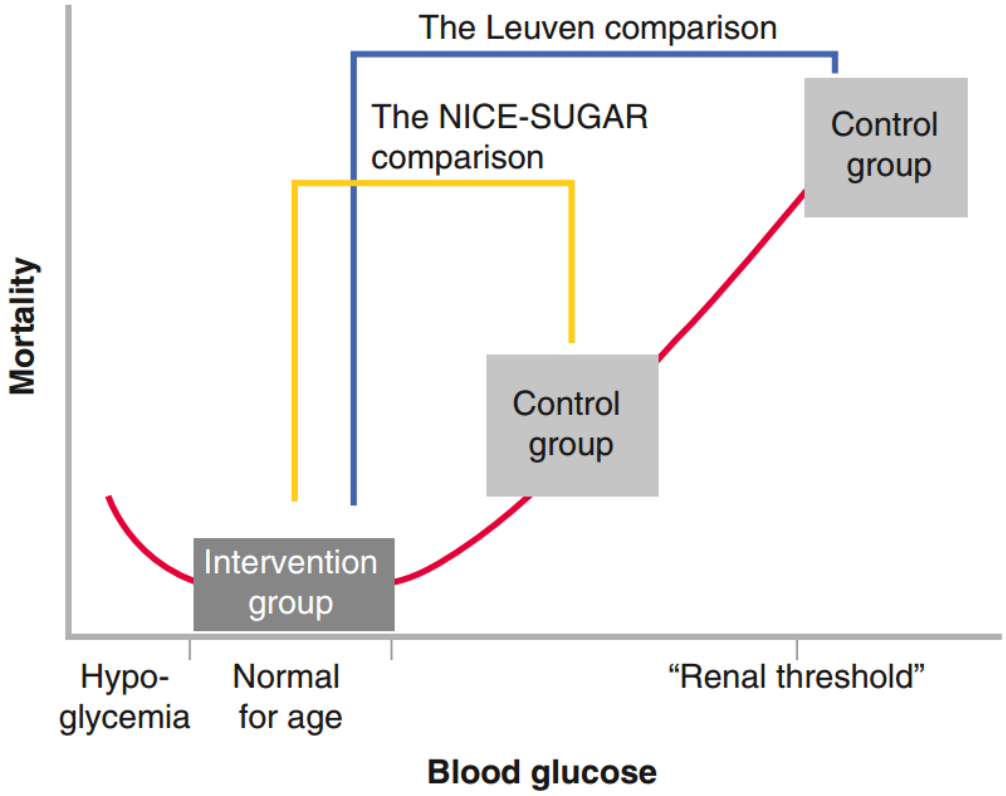

Figure 1.4 Comparison of the Leuven Landmark Study and the NICE-SUGAR Study [Taken from Reference (43)]. The red curve depicts the observed relationship between blood glucose levels and mortality rates in the ICU. “The NICE-SUGAR trial was not a true confirmation study of the Leuven surgical intensive care unit (SICU) study. Despite using similar blood glucose targets for the intervention group, the Leuven SICU study and NICE-SUGAR trail differed in the targets for the control group. Whereas in the Leuven SICU study hyperglycemia up to the renal threshold was accepted, NICESUGAR, already affected by the results from the Leuven SICU study, used an intermediate blood glucose target for the control group” (43).

Figure 1.5 mTOR Complex Regulation and Function.

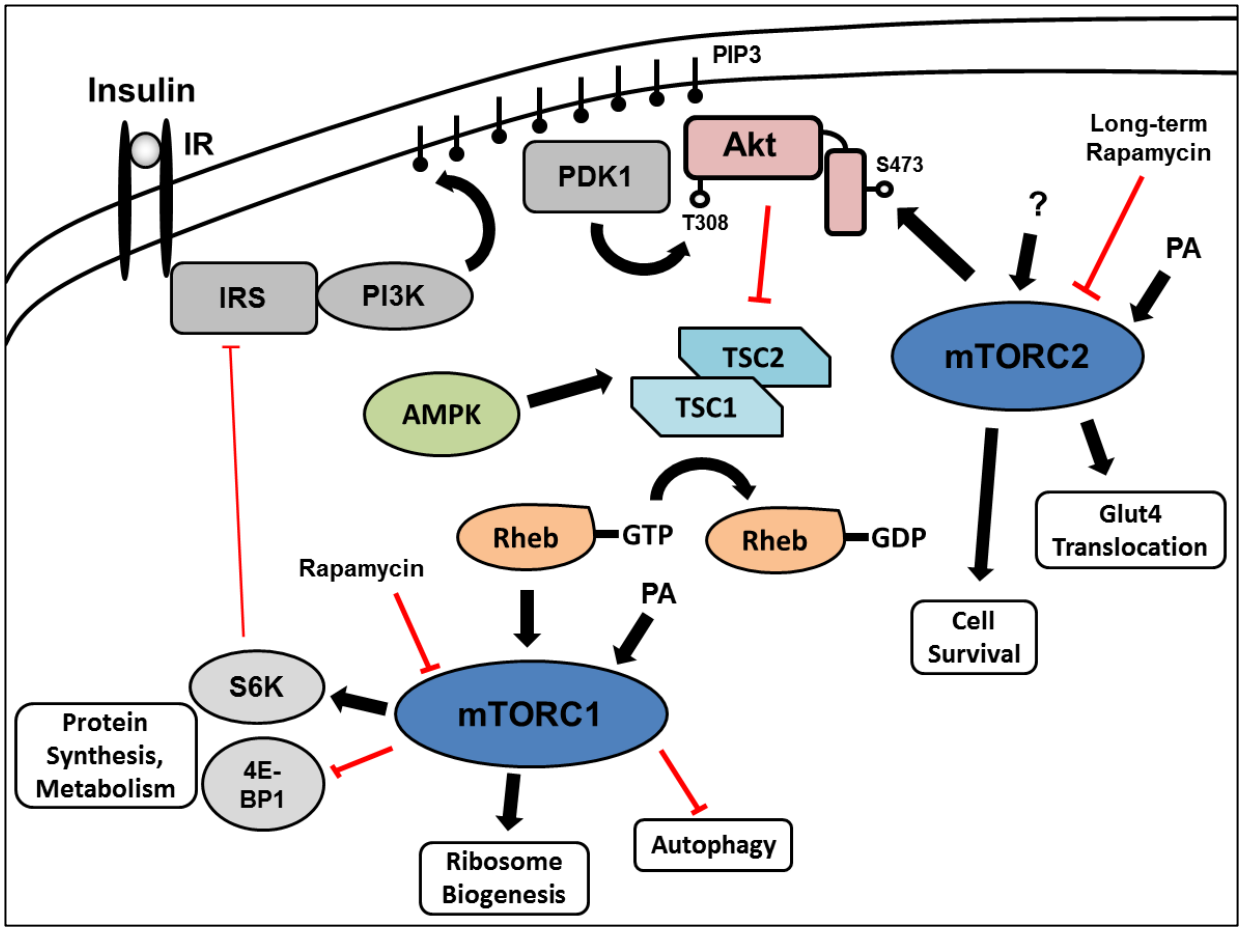

Figure 1.5 mTOR Complex Regulation and Function. Both mTORC1 and mTORC2 are activated by insulin and other growth factors, but the details of mTORC2 activation remain largely unknown. mTORC1 regulation by insulin is very well defined. Briefly, Akt inhibits the TSC2/TSC1 complex by direct phosphorylation of TSC2, and GTP-bound Rheb is increased as a result of this inhibition. GTP-bound Rheb directly interacts with mTORC1, activating the kinase complex. mTORC1 is responsible for initiating protein synthesis, metabolism and ribosome biogenesis, while inhibiting autophagy. mTORC2 plays essential roles in Glut4 translocation to the plasma membrane and promoting cell survival and growth.

CHAPTER 2

EXPERIMENTAL METHODS

Materials

Antibodies to 4E-BP1 and phospho-4E-BP1 T36/45 have been described previously (70). Other antibodies were from the following sources: rictor from Bethyl Laboratories Inc.; FLAG and HA antibodies were from Sigma-Aldrich; and the remaining antibodies were from Cell Signaling Technology. Specifically, the antibodies from Cell Signaling were as follows (given as name of antibody: Cat. No.): mTOR: 2972, pS6K (T389): 9205, Raptor: 2280, HSL: 4107, pHSL (S563): 4139, AS160: 2447, pAS160 (S588): 8730, Akt: 4691, pAkt (S473): 4060, pAkt (T308): 9275, pRaptor (S792): 2083, pIR (Y1150/1151): 3024, IR: 3025, pPKA substrate: 9621, and ATGL: 2138. Forskolin, 8-(4-chlorophenylthio) adenosine 3'-5'-monophosphate (CPT-cAMP), isoproterenol, IBMX, the free glycerol determination kit, microbial lipase, anti-FLAG M2 affinity gel, and all organic solvents were from Sigma-Aldrich. Rapamycin and H-89 were from Calbiochem-Novabiochem. Torin1 was a kind gift from Drs. David Sabatini and Nathaniel Gray. Diethyl-p-nitrophenylphosphate (E600) was from Sigma. Atglistatin and CAY10499 were from Cayman Chemicals. Recombinant human insulin (Humulin R) was from Eli Lilly and Co. [U-^{14}C]-D-glucose was from ICN. [^{3}H]-2-deoxy-D-Glucose and [γ-^{32}P]-ATP were from Perkin Elmer.

Cell Culture

3T3-L1 fibroblasts were grown in Dulbecco's modified Eagle's medium (DMEM, Invitrogen) containing 10% newborn calf serum (Invitrogen). Fibroblasts were converted to adipocytes by

using differentiation medium as described previously (71). Briefly, cells were cultured in Dulbecco's modified Eagle's medium containing 10% fetal bovine serum (FBS, Invitrogen) for 9-12 days after adding the differentiation medium. For experiments, the culture medium was replaced with Dulbecco's modified Eagle's medium containing 1% fetal bovine serum overnight, and the same medium was exchanged before experiments and then incubated at 37 °C with or without forskolin and/or other additions, as indicated.

Western Blot and Quantitative Analysis

Cells were rinsed once with chilled phosphate-buffered saline (145 mM NaCl, 5.4 mM KCl, and 10 mM sodium phosphate, pH 7.4) and then homogenized using a syringe with a 20-gauge needle. Homogenization buffer was composed of buffer A (1 mM EDTA, 1 mM EGTA, 1 mM dithiothreitol, 0.1% Tween 20, 10 mM sodium phosphate, and 50 mM β-glycerophosphate, pH 7.4), supplemented with 1mM phenylmethylsulfonyl fluoride, 10 μg/ml leupeptin, 10 μg/ml aprotinin, 10 μg/ml pepstatin, and 0.5 μm microcystin LR. Homogenates were centrifuged at 16,000 × g for 10 min and supernatant was taken as cell lysate. Lysates were boiled in SDS-loading buffer before SDS-PAGE. Western blotting was carried out as per antibody supplier instructions. Quantitative analysis of western blots represents phosphorylated/total protein for S6K and Akt and phosphorylated/protein loading control for AS160. Blots were imaged by detecting chemiluminescence on a Fujifilm LAS-4000 imager.

mTOR complex Immunoprecipitation

3T3-L1 adipocyte lysates (400 μl for 6-cm dish) were incubated with antibodies (2 μg) bound to protein A-agarose beads (15 μl, for rabbit antibodies) or protein G-agarose beads (15 μl, for

mouse antibodies) at 4 °C for 2 hr with constant mixing. For antibody conjugation to agarose beads, the beads were washed once with water and once with buffer A prior to suspension in 1ml buffer A and addition of antibodies and 0.1% bovine serum albumin (BSA) and rotation for 30 min at room temperature. Cell lysates were added after the antibody supernatant was removed, and the bead/lysate mixture was incubated at 4 °C for 2 hr with constant mixing. After incubation with the lysates the beads were washed with 1 ml of Buffer A plus 0.5 mM NaCl and then twice with 1 ml of Buffer A before elution with SDS sample buffer and SDS-PAGE.

Purification of Recombinant mTOR Complexes

HEK293T cells were transiently transfected with 50 μg of plasmid/15-cm plate using Lipofectamine 2000 at a 2:1 ratio of DNA: Lipofectamine. HA-mTOR and FLAG-raptor plasmids were transfected using 40 and 10 μg of plasmid/15-cm plate, respectively, and 18–24 plates were used for each purification of mTORC1. Each 15-cm plate of cells was lysed in 0.3 ml buffer B (150 mM NaCl, 50 mM Hepes, pH 7.4, 0.4% CHAPS) supplemented with 1mM phenylmethylsulfonyl fluoride, 10 μg/ml leupeptin, 10 μg/ml aprotinin, 10 μg/ml pepstatin, and 0.5 μm microcystin LR, the lysates were cleared by centrifugation at 16,000 × *g* for 10 min, and the supernatant was incubated with anti-FLAG M2 beads (10 μl/ 15-cm plate) for 2 hr at 4 °C. Beads were isolated by centrifugation at 2000 × *g*, and the supernatant was removed. The slurry was packed onto a screening column (Fisher Scientific 11-387-50, 5 ml), washed once with 3 ml buffer B, once with 3 ml wash buffer 1 (150 mM NaCl, 50 mM Hepes, pH 7.4, 0.1% CHAPS), and twice with 1 ml wash buffer 2 (200 mM NaCl, 50 mM Hepes, pH 7.4, 0.1% CHAPS). mTOR complex was eluted by 5 successive additions of an equal volume (200 μl) of elution buffer (500 mM NaCl, 50 mM Hepes, pH 7.4, 0.1% CHAPS) containing 0.5 mg/ml FLAG

peptide (Lifetein). The column was stopped with parafilm for 3 min during the 3rd addition of elution buffer to allow further competitive elution. Elution fractions containing mTORC1 (Generally the first 3) were pooled and dialyzed 3 times against 150 mM NaCl, 50 mM Hepes, 50 mM β-glycerophosphate, pH 7.4. Purified mTORC1 was quantified by comparison of bands of mTOR and raptor to bovine serum albumin standards on Coomassie Blue-stained SDS-PAGE gels.

Lipid Extraction

3T3-L1 adipocytes from 6-cm plates or 100 µl of packed isolated adipocytes were washed twice with PBS, homogenized in 100 µl buffer A (1 mM EDTA, 1 mM EGTA, 1 mM dithiothreitol, 0.1% Tween 20, 10 mM sodium phosphate, and 50 mM β-glycerophosphate, pH 7.4), supplemented with 1 mM phenylmethylsulfonyl fluoride, 10 µg/ml leupeptin, 10 µg/ml aprotinin, 10 µg/ml pepstatin, and 0.5 µM microcystin LR, as well as 20 nM butylated hydroxytoluene (BHT) to prevent lipid oxidation *in vitro* and homogenates were centrifuged at 16,000 × g for 10 min. Supernatant fluid was transferred to a new tube and 400 µl of hexane/ethyl acetate (1:1) was added and mixed for 30 min followed by centrifugation at 8,000 × g for 2 min. The organic phase (top layer) was moved to a new tube, the organic solvent was evaporated in a Thermo Scientific Savant ISS110 Speedvac Concentrator and the lipid residue was either used immediately by re-suspension in buffer, or stored under nitrogen at -80 °C for later use.

In Vitro Fluorescent mTOR Complex Dissociation Assay

Fluorescently-tagged HA-Venus-mTOR/FLAG-Cerulean-Raptor or HA-Venus-mTOR/FLAG-Cerulean-Rictor immune complexes were immobilized by immunoprecipitation with anti-HA antibodies conjugated to Protein-G agarose beads as described under "mTOR Complex Immunoprecipitation". Cleared adipocyte lysate or extracted lipids (50% of a 6-cm plate) were mixed with the fluorescently-tagged mTOR-Raptor or mTOR-Rictor immune complexes on beads for 30 min at room temperature. The amount of mTOR complex in each assay was between 0.9-1.1 μg, which represents approximately 30% of a 15-cm plate of HEK293T cells transfected with mTORC1 or 2 as described above. When using extracted lipids, the dried lipid residue was solubilized in buffer A prior to addition to the immune complexes. The beads were then washed three times, suspended in 100 μl buffer A, transferred to a 96-well plate, and Venus and Cerulean emissions were detected on a TECAN infinite M200. Venus excitation and emission wavelength was 495 nm and 528 nm, respectively, and Cerulean excitation and emission wavelength was 433 nm and 475 nm, respectively. Since it has been established that Triton X-100 will dissociate the mTOR complexes (72), we included 1% Triton X-100 in place of 0.1% Tween-20 in 500 μl buffer A as a positive control for detecting mTOR complex dissociation **(Figure 2.1A)**, and we confirmed the proteins present in the complex at the conclusion of the assay by immunoblotting for raptor and mTOR **(Figure 2.1B)**. The recombinant fluorescently-tagged mTOR-Raptor and mTOR-Rictor complex was generated by transient transfection into HEK293T cells using Lipofectamine 2000 (Invitrogen). HA-Venus-mTOR and FLAG-Cerulean-Raptor/ FLAG-Cerulean-Rictor plasmids were transfected using 40 and 10 μg of plasmid/15-cm plate, respectively, and Lipofectamine 2000 at a 2:1 ratio of DNA: Lipofectamine.

In Vitro mTOR Kinase Assay

250 ng of purified mTORC1 and 1 µg of either 4E-BP1 or S6K were suspended in 25 µl of kinase buffer (50 mM NaCl, 0.1 mM EGTA, 1 mM dithiothreitol, 0.5 µM microcystin LR, 2 mM $MnCl_2$, 10 mM Hepes, and 50 mM β-glycerophosphate, pH 7.4). The kinase reactions were initiated by adding 5 µl of kinase buffer with 3 mM ATP supplemented with [γ-^{32}P]-ATP (PerkinElmer Life Sciences, 1,000 mCi/mmol) for a final ATP concentration of 500 µM. Reactions were incubated for 30 min at 30 °C with consistent shaking and were terminated by the addition of SDS sample buffer. The amounts of ^{32}P incorporation were determined by phosphoimaging after SDS-PAGE. When added, lipids were extracted as described under lipid extraction, solubilized in 100 µl kinase buffer with 0.1% Tween-20 added, and 2 µl was added to the kinase assay. Unless otherwise stated, approximately 2% of the total lipid extracted from a 6-cm plate of 3T3-L1 adipocytes was added per kinase assay.

Lipase Treatment of Lipids *In Vitro*

After lipids were extracted as described under "Lipid Extraction", dried lipid residues were re-suspended in buffer A with or without microbial lipase (2 U/ml) for 30 min at room temperature and lipids were re-extracted and dried as described.

Animal Care

All animals were bred and maintained in accordance with the University of Virginia Animal Care and Use Committee regulations. 8-12 week old ATGL−/− and WT littermate controls on C57BL/6J background were used for studies. Animals were maintained on 12 hr light/ 12 hr dark cycle and had *ad-libitum* access to food (standard rodent chow) and water.

Isolation of Primary Adipocytes

Primary adipocytes were isolated as described previously (26). Briefly, mice were anesthetized by intraperitoneal injection of 0.1 ml/20 g body weight of a mixture of ketamine/ xylazine/ acepromazine in saline, euthanized by cervical dislocation, and epididymal fat pads were removed. Fat pads were added to Krebs Ringer HEPES (KRH) –BSA buffer (with 0.5% insulin-free BSA, and 500 nM adenosine) containing collagenase (type I from Worthington Biochemical Corp., 1 mg/ml, 2 mg/g of tissue). The fat pads in the collagenase solution were minced with scissors and incubated in a 37°C shaking water bath (100 rpm) for 70 min. The fat cells were separated from non-fat cells and undigested debris by filtration through a 0.4 mm Nitex nylon mesh (Tetko) and then washed four times by flotation with KRH-BSA.

Isolation of Primary Hepatocytes

Primary mouse hepatocytes were isolated based on an established protocol (73), seeded in DMEM supplemented with 4.5 g/L glucose, 10% fetal bovine serum, 1 μM dexamethasone and 0.1 μM insulin for 4 h, and cultured overnight prior to experiment in serum-free DMEM with 4.5 g/L glucose, 0.2% bovine serum albumin, 100 nM dexamethasone and 1 nM insulin.

Adipocyte Glucose Uptake

Glucose uptake was measured in isolated adipocytes as described (74). Briefly, isolated adipocytes in KRH-BSA were diluted 10-fold to give an approximate 5% cell suspension. Aliquots of the cell suspension (100 μl) were added to 350 μl of KRH-BSA (0.5% BSA) containing insulin, isoproterenol, and adenosine deaminase as indicated and incubated in a 37 °C shaking water bath (100 rpm) for 30 min. Where indicated, torin1 was added 10 min prior to

these treatments. To each tube, 50 µl of 100 µM [U-^{14}C]-D-glucose in KRH-BSA (1.25 µCi/aliquot) was added, and the incubation continued for another 20 min. Glucose uptake was terminated by separating the medium from the cells in a 200-µl aliquot from each assay tube by centrifugation through 150 µl of dinonyl phthalate in 0.4 ml polyethylene microcentrifuge tubes. After centrifugation, the tubes were cut horizontally through the dinonyl phthalate oil layer and the top half (containing the cell pellet) was moved to a scintillation vial. The cell-associated radioactivity was determined by scintillation counting. Nonspecific association of radioactive glucose with cells was assessed by performing the assay in the presence of cytochalasin B (20 µM). The glucose uptake data were expressed in amoles per minute per cell by calculating cell numbers from lipid weights and adipocyte sizes as described (74). Briefly, cell sizes were measured from cells in a 5% cell suspension using the AMG EVOS fl digital microscope and ImageJ imaging software. For the determination of the lipid content, a 200-µl aliquot of the 5% cell suspension was mixed with 2.7 ml of 40:10:1 isopropanol/heptane/1N H_2SO_4, followed by the addition of 1.8 ml of heptane and 1.0 ml of water. The mixture was vortexed and centrifuged briefly, a 1-ml aliquot of the organic layer was evaporated, and the lipid residue was weighed. Cell area is used to calculate cell volume, which is used in conjunction with lipid content to determine cell number for specific activity.

Measurement of Glycerol and Glycerolipid Release

To measure glycerol release, 3T3-L1 cells were washed twice with DMEM and incubated with DMEM supplemented with forskolin or other additions. For isolated primary adipocytes, media was collected immediately after assay incubation. Glycerol concentration in the media and

glycerolipid levels in adipocyte lipid extracts were measured by free glycerol/glycerolipid determination kit according to manufacturer's instruction (Sigma-Aldrich).

Measurement of Non-Esterified Fatty Acid (NEFA)

NEFAs were measured in adipocyte lipid extracts by HR series NEFA-HR 2 detection kit (Wako Diagnostics) using instructions provided by Mouse Metabolic Phenotyping Centers (MMPC) protocols: http://www.mmpc.org/shared/showFile.aspx?doctypeid=3&docid=196

Liquid Chromatography-Mass Spectrometry

Analysis of DAGs and TAGs was carried out by Liquid Chromatography /Electrospray Ionization Mass Spectrometry (LC/MS) using a triple quadrupole mass spectrometer (Applied Biosystems 4000 Q-Trap) coupled to a Shimadzu LC-20AD LC system equipped with a Discovery (Supelco) C18 column (50mm × 2.1 mm, 5 μm bead size). Analytes were measured in positive mode using ammonium adducts as parent ions and previously described MRMs (75). For oxidized DAGs and TAGs not previously described we used prospective MRMs formulated according with the structure of the oxidized molecules. Mass spectrometer settings were as follows: DP: 71, EP: 10, CE: 33, CXP: 4; Ion spray voltage: 5500; Temperature: 500; Curtain gas; 40. Chromatography was carried out using a mobile phase A consisting of 69% MeOH, 31% Water, 1 mM Ammonium Acetate; and a mobile phase B consisting of 50% MeOH, 50% Isopropanol, 1 mM Ammonium Acetate. The solvent gradient was as follows: 1 min 100% solvent A, a linear gradient to reach 100% solvent B at 8 min, 2 min 100% solvent B, and 2 min 100% solvent A. Total flow was 0.75 ml/min. Quantification was carried out by measuring peak areas using a commercial software (Analyst 1.5.1). When collected from the column for use in

kinase assays, lipid fractions were collected every minute (0.75 ml volume/fraction) for 10 minutes, dried, re-suspended in kinase buffer with 0.1% Tween-20 added, and included in *in vitro* mTOR kinase assays to screen for the presence of the lipid(s) responsible for dissociating the mTOR complexes.

Antioxidant Treatment

6-cm plates of 3T3-L1 adipocytes were incubated with or without ROS scavenger EUK (100 μM), SOD mimic MnTBAP (100 μM), or SOC mimic MnTMPyP (100 μM) for 24 hr followed by treatment with or without forskolin (10 μM) for 45 min. After treatment, cells were washed with chilled phosphate-buffered saline and harvested in buffer A as described under "Western Blot Analysis" and lysates were used for mTOR complex immunoprecipitations and mTOR fluorescent dissociation assays. The media was collected and analyzed for glycerol content to investigate glycerol release.

Tert-Butyl Hydroperoxide Treatment

6-cm plates of 3T3-L1 adipocytes were incubated with or without the lipid soluble oxidizing agent tert-Butyl hydroperoxide (TBH) for 2 hr (1 μM or 10 μM) followed by treatment with or without forskolin (10 μM) for 45 min. After treatment, cells were washed with chilled phosphate-buffered saline and harvested in buffer A as described under "Western Blot Analysis". Lipids were extracted and included in *in vitro* mTORC1 kinase assays as described.

Lipid Reduction by Sodium Borohydride

3T3-L1 adipocytes were treated with or without forskolin (10 μM) for 45 min prior to cell harvest in buffer A and lipid extraction as described. Dried lipids were re-suspended in buffer A with or without the addition of the reducing agent sodium borohydride ($NaBH_4$, 2mM), and incubated for 15 min at room temperature. Lipids were then re-extracted, dried, re-suspended in kinase buffer, and included in mTOR kinase assays.

Lipid Saponification

3T3-L1 adipocytes were treated with or without forskolin (10 μM) for 45 min prior to harvest in buffer A and lipid extraction as described. Dried lipids were re-suspended in buffer A with or without the addition of 200 mM potassium hydroxide (KOH) and incubate at 30 °C for 30 min. Lipids were then re-extracted, dried, re-suspended in either kinase buffer for use in mTOR kinase assays, or buffer A for use in fluorescence mTOR dissociation assays.

Statistical Analysis

Values are expressed as means ± SEM. Data between two groups of similar treatment were compared using Student's t test. Comparisons among >2 groups of similar treatment were done by one-way ANOVA with Dunnett's post hoc analysis (INS set as the control for glucose uptake and insulin signaling western blot quantification, CON set as control for glycerol release, and No Lipid or Vehicle set as control for kinase assays). Comparisons among grouped data were perfomed by two-way ANOVA with Tukey's multiple comparison post hoc analysis (CON set as control in mTOR dissociation assays). Significance is indicated by *, **, ***, or #, for $P<0.05$, 0.01, 0.001, or 0.0001 respectively.

Figure 2.1 mTOR Complex Dissociation *In Vitro.*

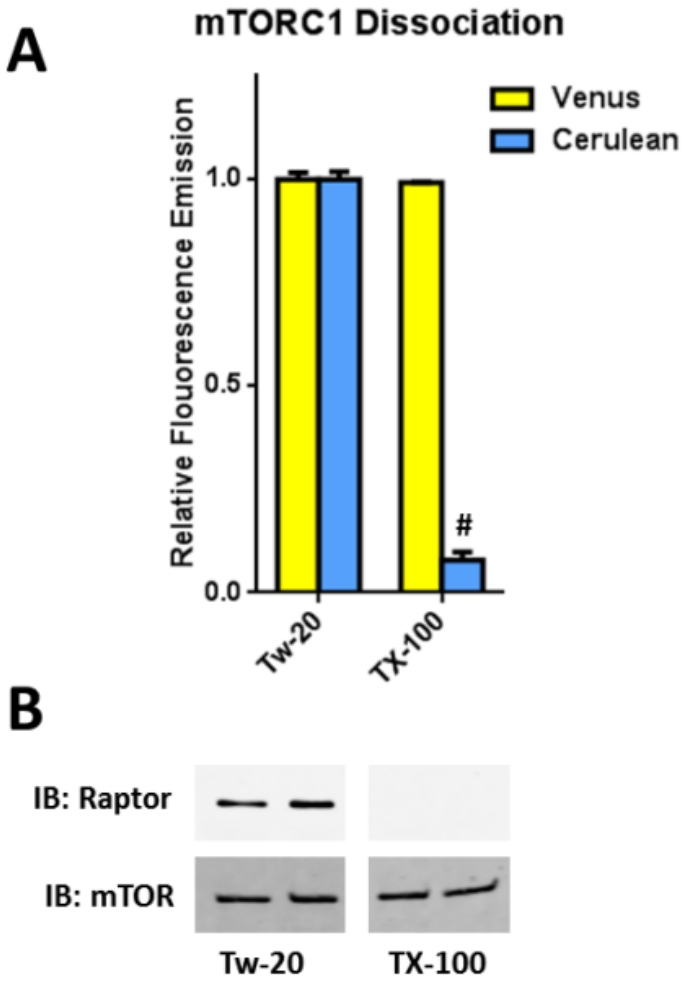

Figure 2.1 mTOR Complex Dissociation *In Vitro.* *A.* mTOR complex 1 dissociation assay performed as described with either 0.1% Tween-20 (Tw-20) or 1% Triton X-100 (TX-100) included in buffer A as detergent. Graph represents mean ± SEM from duplicate experiments. # indicates significant difference from control ($P<0.0001$). *B.* Western blot analysis of the protein present on agarose beads directly after fluorescence detection.

CHAPTER 3

CATECHOLAMINE-INDUCED LIPOLYSIS INHIBITS GLUCOSE UPTAKE THROUGH mTOR COMPLEX DISSOCIATION

ABSTRACT

Anabolic and catabolic signaling oppose one another in adipose tissue to maintain cellular and organismal homeostasis, but these pathways are often dysregulated in metabolic disorders. Although it has long been established that stimulation of the β-adrenergic receptor inhibits insulin-stimulated glucose uptake in adipocytes, the mechanism has remained unclear. Here we report that β-adrenergic-mediated inhibition of glucose uptake requires lipolysis. We also show that lipolysis suppresses glucose uptake by inhibiting the mTOR complexes 1 and 2 through complex dissociation. In addition, we show that products of lipolysis inhibit mTOR through complex dissociation *in vitro*. These findings reveal a previously unrecognized intracellular signaling mechanism whereby lipolysis blocks the PI3K-Akt-mTOR pathway, resulting in decreased glucose uptake. This novel mechanism of mTOR regulation likely contributes to the development of insulin resistance.

INTRODUCTION

Adipose tissue plays an essential role in maintaining whole-body energy homeostasis by storing or releasing nutrients. This balance is controlled by opposing signaling pathways where anabolic processes are activated by insulin and catabolic actions are activated by catecholamines. An important unanswered question in adipose tissue biology is how catecholamine-induced β-adrenergic signaling opposes insulin-stimulated glucose uptake (14-19). Surprisingly, the underlying mechanism for this well-established physiological response in adipocytes is still unknown.

When nutrients are plentiful, insulin is released by the pancreas and stimulates the absorption of glucose and fatty acids in adipocytes, where they are packaged and stored as TAG in cellular lipid droplets. Insulin signaling in adipocytes is mediated by the PI3K-Akt-mTOR pathway. mTOR is a highly conserved Serine/Threonine protein kinase that functions in either of two distinct multi-protein complexes, mTORC1 and mTORC2. mTORC1 is defined primarily by the association of mTOR with raptor, whereas mTORC2 includes mTOR with rictor (76). Importantly, mTORC2 phosphorylation of Akt at S473 is required for Akt activity on AS160, which is necessary for glucose uptake in response to insulin (22, 26, 60, 61). Of note, for both mTORC1 and mTORC2, the integrity of these protein complexes is essential for kinase substrate specificity and proper signaling (52, 62).

During periods of fasting or stress, catecholamines are released by the sympathetic nervous system to activate lipolysis. Stimulation of the β-adrenergic receptor on adipocytes activates AC, leading to elevated cAMP and PKA activity. PKA initiates lipolysis by direct phosphorylation of HSL and perilipin (1-3) and indirect activation of ATGL (4, 8, 77). Lipolysis involves hydrolysis of TAG stored in the lipid droplet to produce DAG, MAG, fatty acids, and

glycerol. These lipolytic products are important energy substrates that can act as precursors for other lipids and impact cellular signaling. However, their role as signaling molecules has not been sufficiently investigated (10).

In this chapter, we provide new insights into the mechanisms that link β-adrenergic stimulation to the inhibition of insulin-stimulated glucose uptake. Namely, we show that activation of lipolysis is crucial. Moreover, we find that products of lipolysis themselves cause mTOR inhibition by complex dissociation, which inhibits glucose uptake in adipocytes. This novel mechanism of mTOR regulation (i.e., by complex dissociation) has major implications in the regulation of cellular metabolism and likely contributes to stress-induced hyperglycemia and obesity-induced insulin resistance.

RESULTS

Catecholamine-Induced Inhibition of Glucose Uptake and Insulin Signaling Requires Lipolysis. Mice lacking ATGL show improved glucose tolerance and are resistant to high-fat diet-induced insulin resistance (27, 78, 79). ATGL deficiency also improves insulin signaling in white adipose tissue (78). These observations implicate lipolysis in insulin resistance. In addition, stimulation of the β-adrenergic receptor in isolated adipocytes is known to acutely inhibit insulin-stimulated glucose uptake (14, 15, 17). To investigate a possible role for lipolysis in the effects of catecholamine action, we compared glucose uptake in WT and *Atgl*-/- primary mouse adipocytes during treatment with isoproterenol, a β-adrenergic receptor agonist. As previously reported, isoproterenol inhibited glucose uptake in WT adipocytes; however, here we show that this inhibition was rescued in the absence of ATGL **(Figures 3.1A and E).** As expected, lipolysis was effectively blocked in *Atgl*-/- adipocytes even during treatment with isoproterenol **(Figure 3.1F).** Rescue of glucose uptake was also observed in cultured 3T3-L1 adipocytes on lipase inhibition with E600, a general lipase inhibitor that binds irreversibly to the active site of lipases **(Figure 3.1G).** In addition, insulin signaling necessary for GLUT4 translocation was restored in the *Atgl*-/- adipocytes as compared to WT **(Figures 3.1B, C, and D)**. Taken together, these data show that lipolysis is required for catecholamine-mediated inhibition of glucose uptake in adipocytes.

The β-Adrenergic/cAMP Pathway Impairs Insulin Signaling by Inhibiting the mTOR Complexes. Similar to isoproterenol-mediated inhibition of glucose uptake, treating adipocytes with forskolin, a potent activator of AC, inhibits insulin signaling (18, 19). We found that forskolin action significantly inhibited mTORC1 and 2 in response to insulin as measured by phosphorylation of S6K (T389) and Akt (S473), respectively **(Figures 3.2A and B).** Although

signaling downstream of the mTOR complexes was inhibited, upstream signaling was unaffected, as shown by tyrosine phosphorylation of the insulin receptor and PDK1-mediated phosphorylation of Akt at T308 **(Figure 3.2A).** Analogous results were observed in primary rat adipocytes treated with isoproterenol prior to insulin stimulation **(Figures 3.2C and D),** and the inhibition of AS160 in both cultured 3T3-L1 and primary rat adipocytes **(Figures 3.2A and C)** demonstrates that AC activity plays a role in dampening glucose uptake. The effects of AC activity on mTOR were reiterated by treatment with a membrane permeable cAMP analog cpt-cAMP, the phosphodiesterase (PDE) inhibitor IBMX, and isoproterenol, demonstrating that elevated cAMP is sufficient to inhibit mTOR in adipocytes **(Figures 3.2E and F).** Activation of adipocyte lipolysis was measured by phosphorylation of HSL **(Figures 3.2A, C, and E)** and glycerol release **(Figures 3.2G and H).** In addition, treatment with forskolin had no effect on phosphorylation of raptor by AMPK **(Figure 3.2I).** Interestingly, forskolin does not inhibit insulin signaling in 3T3-L1 fibroblasts prior to differentiation into adipocytes or in primary mouse hepatocytes **(Figure 3.2J).** Taken together, these data demonstrate that cAMP activity inhibits mTOR in adipocytes, which may play a role in the observed catecholamine-induced decrease in glucose uptake.

cAMP-Mediated Inhibition of mTOR Requires PKA and Lipase Activity. The primary role of cAMP in adipocytes is to activate PKA, which leads to lipolysis through lipase activation and phosphorylation of perilipin (1-3). To investigate the mechanism of cAMP-mediated inhibition of mTOR, we pharmacologically inhibited PKA during forskolin and insulin treatment. The ATP-competitive PKA inhibitor, H89, greatly inhibited PKA activity and rescued both mTORC1 and 2 activity in response to insulin **(Figures 3.3A and C).** In addition, blocking lipase action with E600; atglistatin, a specific ATGL inhibitor; or CAY10499, a specific HSL

inhibitor, reversed the cAMP-mediated inhibition of mTOR **(Figures 3.3B and C)**. Interestingly, we found that blocking lipase action induced S6K phosphorylation during treatment with forskolin **(Figure 3.3B),** but adipocytes have consistently shown mTORC1 inhibition in response to elevated cAMP (80-82). This seemingly paradoxical trend may be similar to cAMP activation of mTORC1 in other cell types (83), when the inhibitory effects of lipolysis are absent. Lipase inhibition also blocked lipolysis as measured by glycerol release **(Figure 3.3D).** Taken together, these data demonstrate that elevated cAMP acts through PKA and activation of lipolysis to disrupt mTOR activity in adipocytes.

Lipolytic Products Inhibit mTOR Activity In Vitro. Lipolysis produces DAG, MAG, fatty acid, and glycerol through lipase action on TAG. To determine if these lipolytic products are responsible for lipolysis-mediated inhibition of mTOR, we examined their ability to inhibit purified recombinant mTOR **(Figure 3.4A)** *in vitro*. We extracted lipids from adipocytes treated with or without the lipolytic agents forskolin or isoproterenol, and included these lipids in mTOR kinase assays. We show that lipids extracted from cultured adipocytes undergoing lipolysis consistently inhibited mTOR, while lipids from control cells had no effect **(Figure 3.4B).** Lipids extracted from WT primary mouse adipocytes showed similar results; however, lipids from either control or isoproterenol treated *Atgl*-/- mouse adipocytes had no effect on mTOR **(Figure 3.4C).** Importantly, although the lipids extracted from control cells did not inhibit mTOR, treating these lipids with a lipase *in vitro* did generate inhibitory lipids **(Figure 3.4D).** To investigate what lipids may be responsible for inhibiting mTOR, we included specific fatty acids or glycerolipids in the mTOR kinase assay. These showed no significant effect on mTOR activity **(Figure 3.4E),** suggesting that it may be a particular lipid released during lipolysis and not lipolytic products in general that inhibit mTOR. To verify the kinase activity was solely due

to purified mTOR, we show complete inhibition by Torin1 **(Figure 3.4F),** and kinetic analysis of mTORC1 activity *in vitro* **(Figure 3.4G).** These data demonstrate that lipolytic products inhibit mTOR *in vitro,* suggesting that they may facilitate catecholamine-induced inhibition of glucose uptake in adipocytes.

Lipolytic Products Inhibit mTOR through Complex Dissociation. In our attempts to purify mTOR from adipocytes, we observed that the mTOR complexes 1 and 2 were dissociated in cells treated with forskolin as compared to control **(Figures 3.5A and B).** Similar to the rescue of mTOR signaling shown in Figures 3.3B and 3.3C, atglistatin rescued mTORC1 and 2 dissociation in cultured adipocytes **(Figure 3.5C),** suggesting that the mechanism of forskolin-induced mTOR inhibition occurs through mTOR complex dissociation. Complementary to the glucose uptake and insulin signaling data in Figures 3.1, mTORC2 dissociation was also observed in WT and rescued in *Atgl*-/- primary mouse adipocytes **(Figure 3.5D).** These data demonstrate that lipolysis is required for the observed mTOR complex dissociation. In addition, lipid extracts from cultured adipocytes treated with forskolin caused mTOR complex dissociation *in vitro*, while lipids from vehicle-treated adipocytes had no effect on the complex **(Figure 3.5E).** To quantitatively show mTOR dissociation *in vitro,* we purified a fluorescently-tagged mTOR complex composed of a Venus-tagged mTOR and a Cerulean-tagged raptor or rictor **(Figure 3.5F).** This recombinant mTOR complex was useful because fluorescent protein tags can be spectrophotometrically detected. In our mTOR dissociation assay, the detected Venus or Cerulean emission directly represents the presence of mTOR or raptor/rictor, respectively **(Figure 3.5G),** and dissociation can be efficiently and quantitatively determined *in vitro*. We used this assay to show that lipids extracted from adipocytes treated with forskolin dissociate mTORC1 and 2 *in vitro,* while lipids extracted from untreated cells, metabolites that partition to

the aqueous phase, or lipids from 3T3-L1 fibroblasts prior to differentiation or primary hepatocytes have no effect **(Figure 3.5H).** Complementary to the insulin signaling shown in Figures 3.3B and 3.3C, lipase inhibition also blocked the dissociation of mTOR **(Figure 3.5I).** Lipids produced from *in vitro* lipase treatment of adipocyte cell extracts also caused mTOR dissociation, while vehicle-treated lipids did not **(Figure 3.5J).** Taken together, these data show that lipolytic products facilitate mTOR inhibition through mTOR complex dissociation.

Torin1-Induced Inhibition of Glucose Uptake is Independent of Lipolysis. mTOR activity is necessary to facilitate insulin-induced glucose uptake in adipocytes (22, 26, 60, 61). Here we show that isoproterenol stimulation of the β-adrenergic receptor and direct mTOR inhibition by Torin1 inhibit glucose uptake in WT primary mouse adipocytes, whereas direct mTOR inhibition alone is sufficient to block glucose uptake in the absence of ATGL **(Figure 3.6A).** In addition, while stimulation of the β-adrenergic receptor only inhibits insulin signaling in WT adipocytes **(Figures 3.1B, C and D),** Torin1 inhibits insulin signaling in both WT and *Atgl*-/- adipocytes **(Figure 3.6B).** Taken together, these data suggest that mTOR inhibition by lipolysis is a likely mechanism of catecholamine-induced inhibition of glucose uptake in adipocytes.

DISCUSSION

The major finding of this study is that lipolysis acutely inhibits insulin-stimulated glucose uptake in adipocytes. The ability of catecholamines to dampen adipocyte glucose uptake has been known for decades and documented repeatedly (14, 15, 17-19). Here we not only show that lipolysis is required to mediate this inhibition of glucose uptake, but that the mechanism of inhibition may be through dissociation of the mTOR complexes and subsequent inhibition of insulin-stimulated Akt activity. Interestingly, mTOR signaling and complex association are rescued when lipolysis is inhibited, and lipolytic products that partition to the organic phase are able to directly dissociate mTOR *in vitro,* suggesting that these lipids can act as signaling molecules to regulate insulin action. Lipolytic products produced *in vitro* also inhibit mTOR through dissociation, suggesting that further enzymatic activity is not required for lipolysis to mediate these effects on mTOR. Although it has recently been shown that lipolytic products can activate peroxisome proliferator-activated receptor (PPAR) α and δ (84), potentially impacting insulin signaling through PTEN expression, our finding that insulin signaling upstream of mTOR is unaffected by lipolysis suggests this is not the mechanism of insulin resistance in our model.

Lipotoxicity is one of the hypotheses being explored to explain the mechanisms by which obesity induces insulin resistance. Also known as the lipid metabolite theory, lipotoxicity is characterized by an excess of lipids that can act as signaling molecules to inhibit insulin signaling (30-32). Previous data have shown that insulin resistance is often associated with lipid accumulation in liver and skeletal muscle, and high levels of circulating lipolytic products may correlate with obesity and insulin resistance in type 2 diabetes (85, 86). Importantly, lipid accumulation in the liver has been shown to inhibit insulin signaling specifically by decreasing mTORC2 complex integrity and activity (63). In addition, levels of basal lipolysis are elevated

during obesity (9, 87) and decreased lipolysis due to lipase deficiency in mice attenuates diet-induced insulin resistance (27, 28). Taken together, these observations implicate lipolytic products in the development of insulin resistance, and here we demonstrate that lipids released during lipolysis have local effects on mTOR signaling and insulin-stimulated glucose uptake in adipocytes.

Although insulin resistance depends on insulin action in multiple tissues, adipocyte-specific GLUT4-/- mice develop systemic insulin resistance and hyperglycemia (25) while adipocyte-specific GLUT4 overexpression results in enhanced insulin sensitivity *in vivo* (88). As previously stated, this indicates that impaired insulin action in adipocytes alone is sufficient to drive whole-body insulin resistance and hyperglycemia. Our previous work also demonstrates that impaired insulin action due to decreased rictor expression in adipocytes results in whole-body insulin resistance and hyperglycemia (26). Taken together with data shown in this chapter, these findings suggest mTOR complex inhibition as an acutely-regulated event that leads to impaired insulin signaling in adipocytes, which may have an impact on the development of systemic insulin resistance. This study also demonstrates a novel mechanism of mTOR complex dissociation and inhibition by lipolytic products. Our proposed mechanism highlights the importance of lipolysis in regulating cellular signaling events, as a potential consequence of releasing energy stores.

In addition to mechanistic details of the opposing actions of anabolic and catabolic signaling in adipose tissue, our findings directly implicate lipolysis as the mechanism underlying adipocyte insulin resistance during acute stress events and may provide insight into obesity-induced insulin resistance. Acute hyperglycemia often develops after trauma or major surgery, particularly surgery within the abdominal cavity (33), after severe burn injuries, or sepsis. If

untreated, stress-induced hyperglycemia contributes to mortality and delays healing in post-surgery and ICU patients (34). Although the effects of stress on insulin action are well known, the mechanistic link has remained unclear. Our finding that lipolysis plays a key role in decreasing insulin signaling suggests that it may be a contributing factor in the development of stress-induced hyperglycemia.

In obese humans, while catecholamine stimulation of lipolysis is sometimes dampened, basal levels of lipolysis are commonly elevated. Therefore, in addition to the acute events investigated within this report, it is intriguing to consider the role of lipolysis and inhibition of the mTOR signaling pathways in adipocytes in the development of obesity-induced insulin resistance over time. In addition to β-adrenergic stimulation, lipolysis is elevated by inflammatory cytokines, natriuretic peptides, growth hormones, and cortisol (89), highlighting that many factors could be contributing to this mechanism of insulin resistance. Although we have shown that acute stimulation of lipolysis may inhibit glucose uptake through mTOR complex dissociation, further investigation is necessary to determine the contribution of lipolysis to obesity-induced insulin resistance.

In this study, we have identified a novel mechanism of adipocyte signaling whereby lipolytic products dissociate the mTOR complexes, resulting in decreased insulin-stimulated glucose uptake **(Figure 3.6C).** This model has implications in obesity-induced insulin resistance and stress-induced hyperglycemia and demonstrates that lipolytic products can function as signaling molecules to regulate cellular processes. It also provides new insight into the mechanisms of opposing regulation between anabolic and catabolic signaling in adipocytes.

Figure 3.1 Catecholamine-Induced Inhibition of Glucose Uptake and Insulin Signaling Requires Lipolysis.

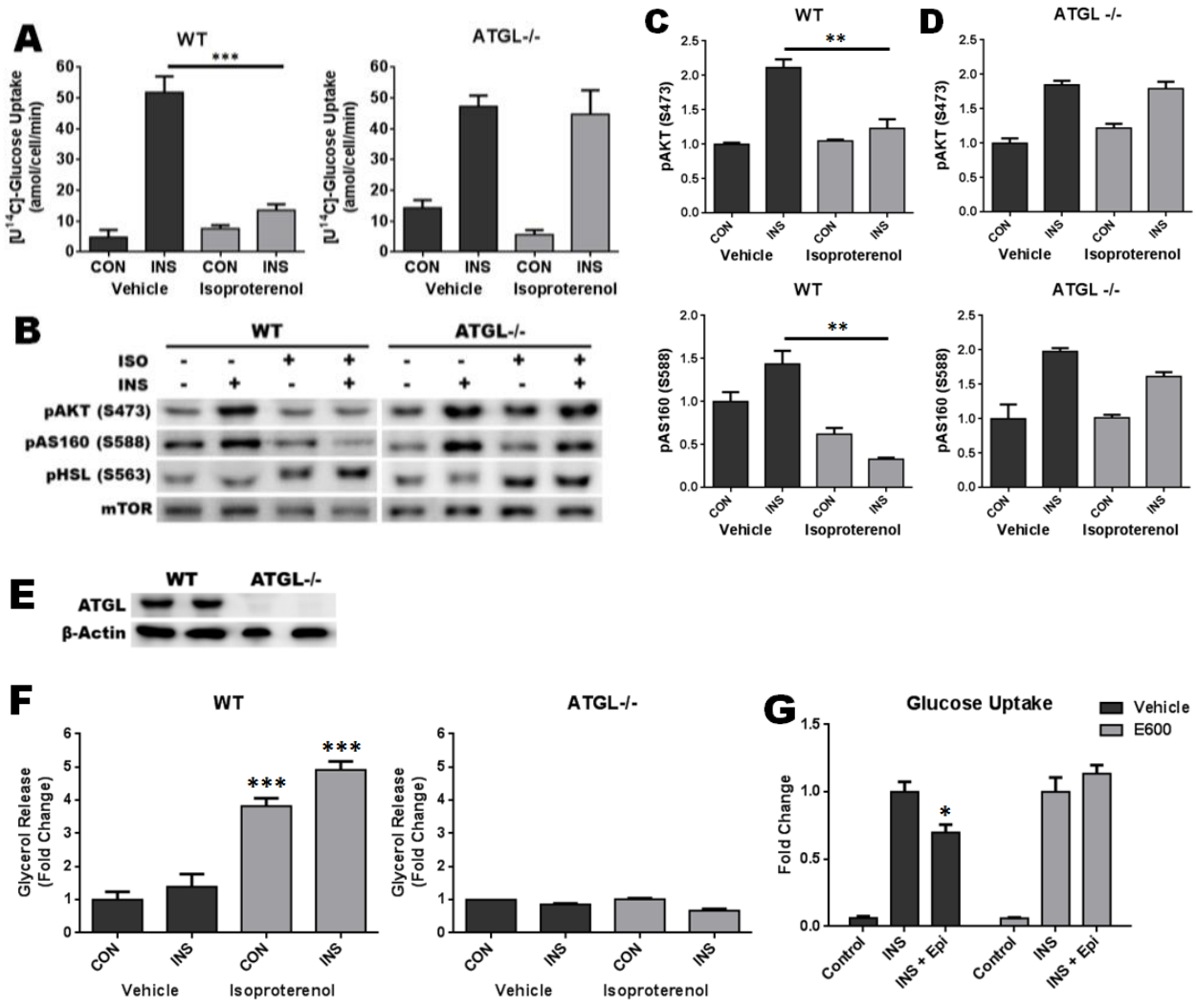

Figure 3.1 Catecholamine-Induced Inhibition of Glucose Uptake and Insulin Signaling Requires Lipolysis. *A*. Radiolabeled glucose uptake assays in WT vs *Atgl* -/- primary mouse adipocytes. Isolated adipocytes were treated with or without insulin (10 nM) in the presence or absence of isoproterenol (0.1 μM) for 30 min followed by [U-^{14}C]-D-Glucose (10 μM) for 20 min before assay termination. All assays contained adenosine deaminase (ADA, 2 U/ml). *B*. Western blot analysis of insulin signaling in WT and *Atgl* -/-primary mouse adipocytes treated as in Figure 3.1*A*. *C*. Quantitative analysis of insulin signaling in WT adipocytes from Figure 3.1*B*. *D*. Quantitative analysis of insulin signaling in *Atgl* -/- adipocytes from Figure 3.1*B*. *E*. Western blot analysis of WT and *Atgl* -/- primary mouse adipocytes. *F*. Glycerol release from WT and *Atgl* -/- primary mouse adipocytes treated as in Figures 3.1*A* and 3.1*B* before the addition of glucose. *G*. [^{3}H]-2-deoxy-D-glucose uptake in cultured 3T3-L1 adipocytes treated with or without insulin (10 nM) and epinephrine (Epi, 10 μM) for 30 min in the presence or absence of diethyl-p-nitrophenylphosphate (E600, 150 μM). Each graph represents mean ± SEM from triplicate experiments. Asterisk indicates significant difference ($P<0.05$, $P<0.01$, or $P<0.001$ for *, **, or ***, respectively).

Figure 3.2 The β-Adrenergic/cAMP Pathway Impairs Insulin Signaling by Inhibiting the mTOR Complexes.

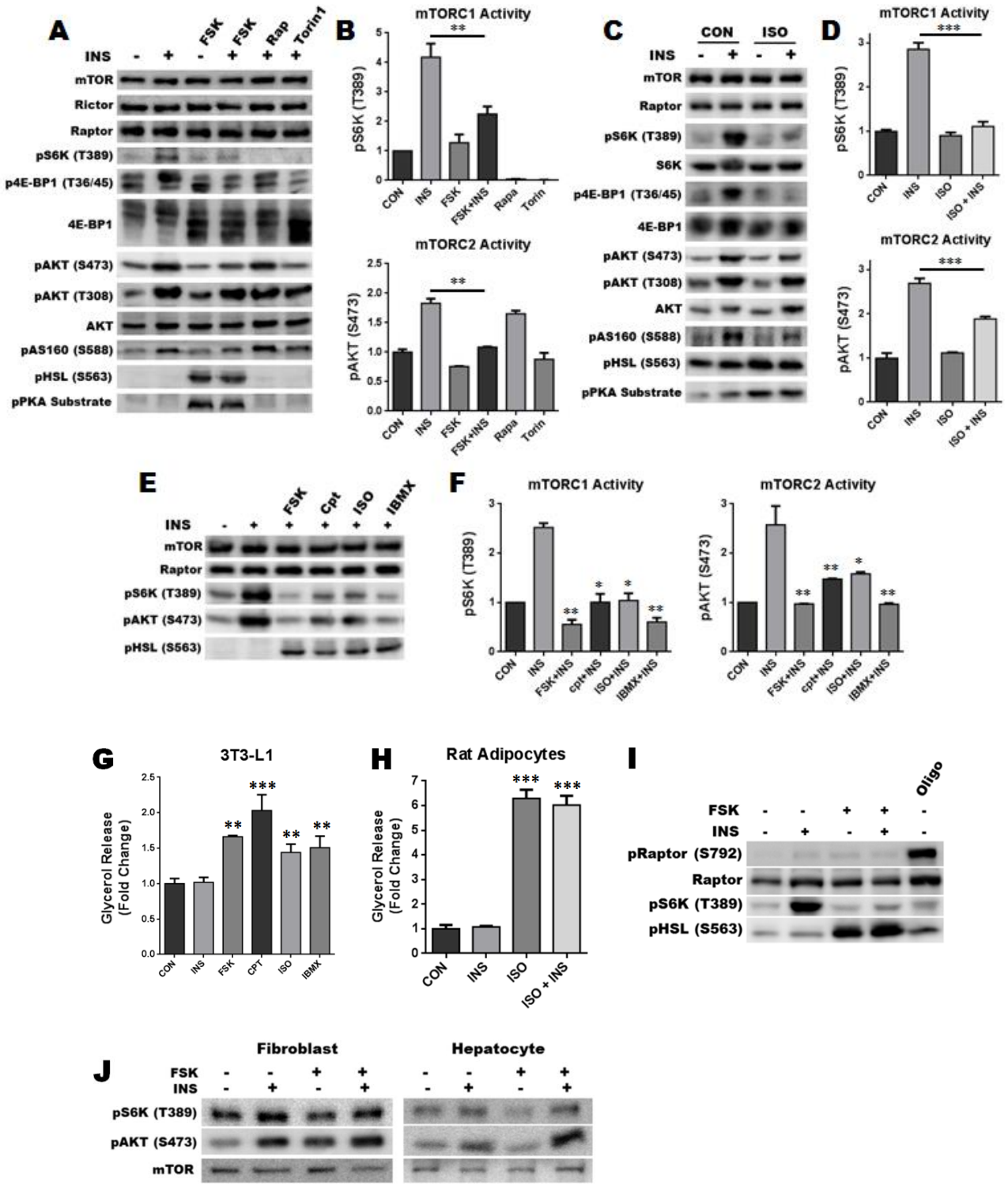

Figure 3.2 The β-Adrenergic/cAMP Pathway Impairs Insulin Signaling by Inhibiting the mTOR Complexes. *A*. Western blot analysis from cultured 3T3-L1 adipocytes treated with or without forskolin (FSK, 10 μM), Rapamycin (Rap, 20 nM), or Torin1 (250 nM) for 30 min prior to insulin treatment (INS, 10 nM) for 15 min. *B*. Quantitative analysis of pS6K (T389) and pAKT (S473) from Figure 3.2*A* to show mTORC1 and mTORC2 activity, respectively. *C*. Western blot analysis of insulin signaling in primary rat adipocytes treated with or without isoproterenol (ISO, 10 μM) for 30 min prior to treatment with or without insulin (10 nM) for 15 min. *D*. Quantitative analysis of pS6K (T389) and pAKT (S473) from Figure 3.2*C*. *E*. Western blot analysis of insulin signaling cascades in cultured 3T3-L1 adipocytes. Adipocytes were treated with or without forskolin (FSK, 10 μM), Cpt-cAMP (Cpt, 100 μM), isoproterenol (ISO, 5 μM), or IBMX (200 μM) prior to insulin treatment (INS, 10 nM) for 15 min. *F*. Quantitative analysis of pS6K (T389) and pAKT (S473) from Figure 3.2*E*. *G*. Glycerol release from cultured 3T3-L1 adipocytes treated as in Figure 3.2*E*. *H*. Glycerol release from primary rat adipocytes treated as in Figure 3.2*C*. *I*. Western blot analysis of cultured 3T3-L1 adipocytes treated with or without forskolin (FSK, 10 μM) or the AMPK activator oligomycin (Oligo, 1 μM) for 30 min prior to insulin treatment (INS, 10 nM) for 15 min. *J*. Western blot analysis of insulin signaling in cultured undifferentiated fibroblasts and isolated mouse hepatocytes treated with or without forskolin (FSK, 10 μM) for 30 min prior to insulin treatment (INS, 10 nM) for 15 min. Each graph represents mean ± SEM from triplicate experiments. Asterisk indicates significant difference ($P<0.05$, $P<0.01$, or $P<0.001$ for *, **, or ***, respectively).

Figure 3.3 cAMP-Mediated Inhibition of mTOR Requires PKA and Lipase Activity.

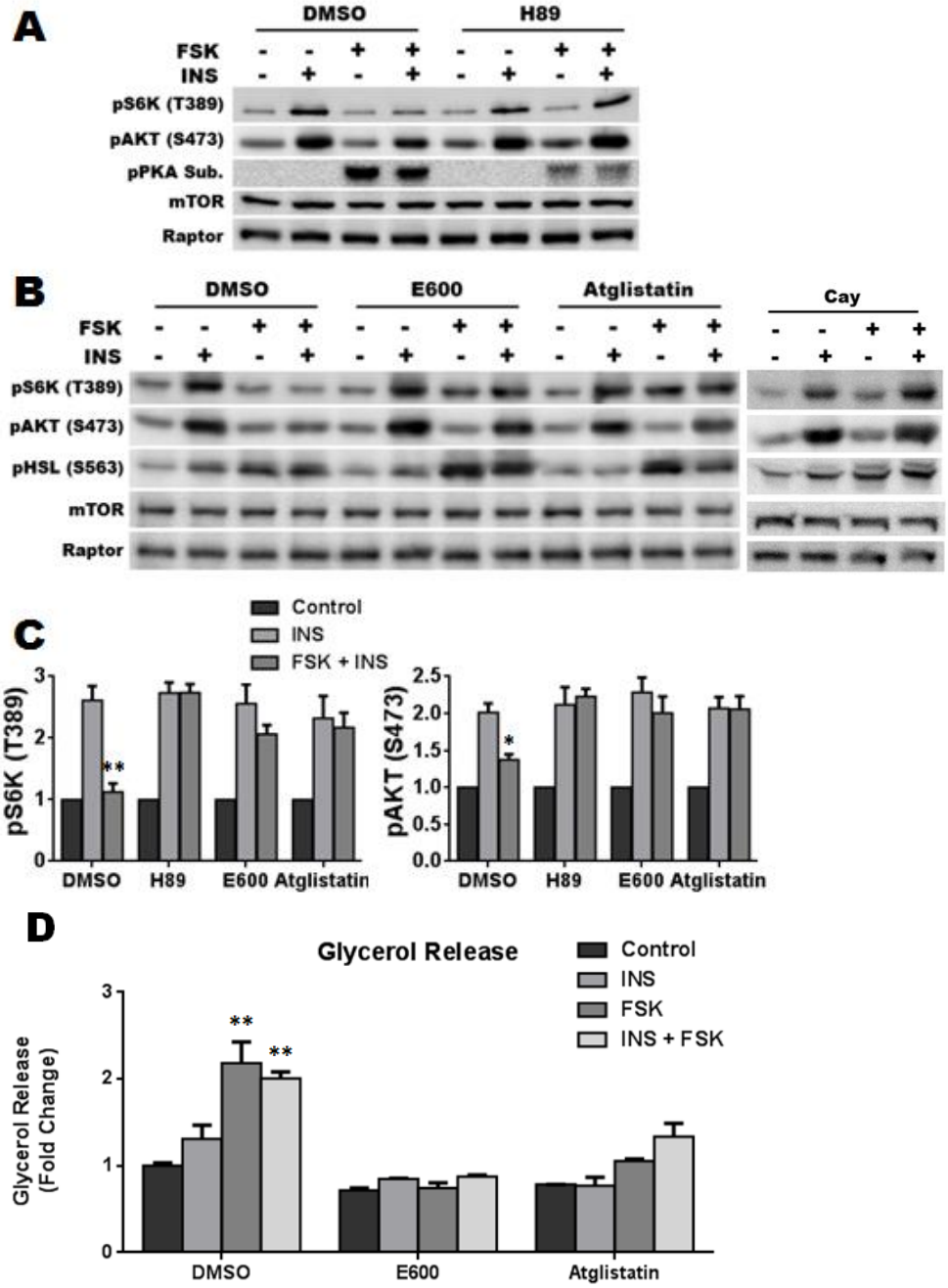

Figure 3.3 cAMP-Mediated Inhibition of mTOR Requires PKA and Lipase Activity. *A.* Western blot analysis of cultured 3T3-L1 adipocytes pre-treated with the PKA inhibitor, H89 (10 μM) for 20 min prior to treatment with or without forskolin (FSK, 10 μM) for 30 min followed by insulin treatment (INS, 10 nM) for 15 min as in Figure 3.2*A. B.* Western blot analysis from cultured 3T3-L1 adipocytes pre-treated with the general lipase inhibitor, diethyl-p-nitrophenylphosphate (E600, 150 μM), the specific ATGL inhibitor, Atglistatin (10 μM), or the specific HSL inhibitor CAY10499 (Cay, 2 μM) for 1 hr prior to forskolin and insulin treatment as in Figure 3.3*A. C*. Quantitative analysis of pS6K (T389) and pAKT (S473) from experiments in Figures 3.3*A* and 3.3*B. D.* Analysis of glycerol release from cultured 3T3-L1 adipocytes from Figure 3.3*B.* Each graph represents mean ± SEM from triplicate experiments. Asterisk indicates significant difference ($P<0.05$ or $P<0.01$ for * or ** respectively).

Figure 3.4 Lipolytic Products Inhibit mTOR Activity *In Vitro*.

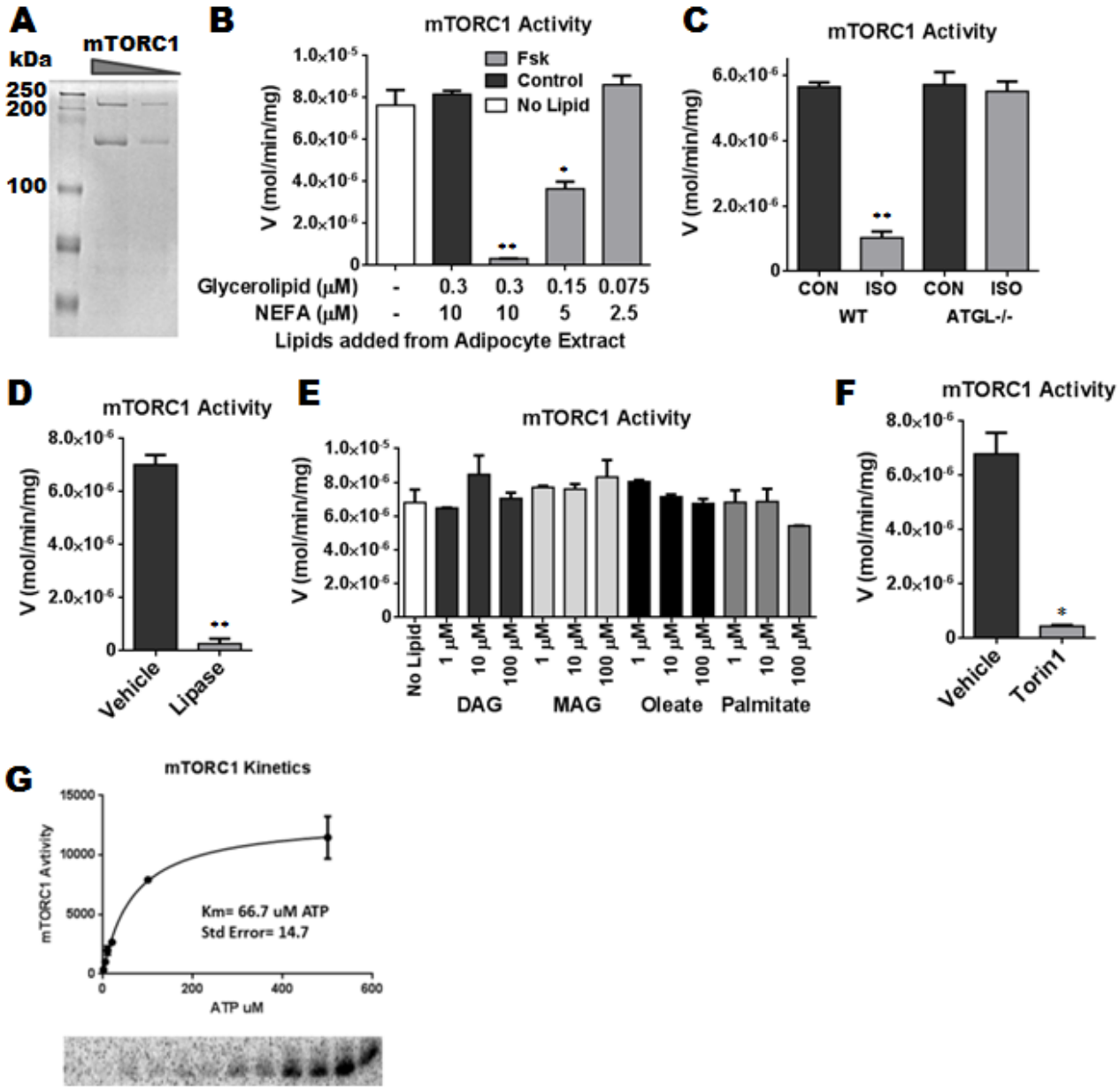

Figure 3.4 Lipolytic Products Inhibit mTOR Activity *In Vitro*. *A.* Coomassie stain of recombinant mTORC1 purification showing mTOR (upper band) and raptor (lower band). *B.* Radioactive *in vitro* mTOR kinase assays using purified recombinant mTORC1 and 4E-BP1 as substrate. No lipid vehicle or lipids extracted from cultured 3T3-L1 adipocytes treated with or without forskolin (Fsk, 10 μM) for 30 min were added to the assay 10 min prior to the addition of [γ-^{32}P]-ATP. *C.* mTOR kinase assays as in Figure 3.4*B* using lipids extracted from WT or *Atgl* -/- primary mouse adipocytes after treatment with or without isoproterenol (ISO, 10 μM) for 30 min. *D.* mTOR kinase assays as in Figure 3.4*B* using lipids extracted from cultured 3T3-L1 adipocytes. The lipids were treated with or without lipase *in vitro* prior to adding them to the mTOR kinase assay. *E.* mTOR kinase assays as in Figure 3.4*B* where 1-palmitoyl-2-oleoyl-sn-glycerol (DAG), 2-oleoyl-glycerol (MAG), oleate, or palmitate were added as indicated. *F.* Radioactive *in vitro* mTOR kinase assay as in Figure 3.4*B* in the presence or absence of the mTOR inhibitor, Torin1 (250 nM) using 4E-BP1 as substrate. *G.* Kinetic analysis of mTORC1 kinase activity *in vitro* using 4E-BP1 as substrate. Each graph represents mean ± SEM from triplicate experiments. Asterisk indicates significant difference ($P<0.05$ or $P<0.01$ for * or ** respectively).

Figure 3.5 Lipolytic Products Inhibit mTOR through Complex Dissociation.

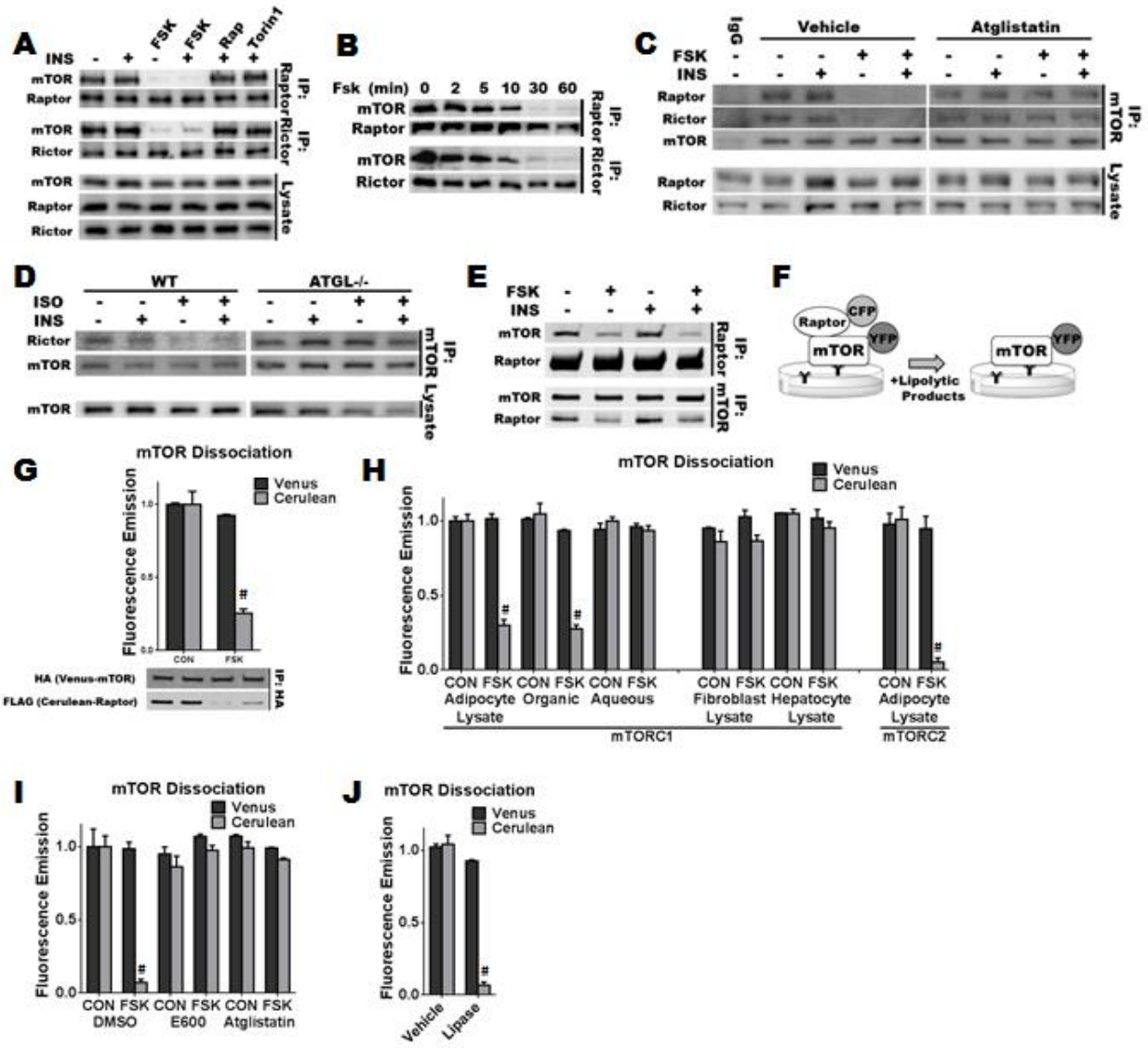

Figure 3.5 Lipolytic Products Inhibit mTOR through Complex Dissociation. *A.* Western blot analysis of mTORC1 and mTORC2 co-immunoprecipitations against raptor and rictor, respectively, where cultured adipocytes were treated with or without forskolin (FSK, 10 μM), Rapamycin (Rap, 20 nM), or Torin1 (250 nM) for 30 min prior to insulin treatment (INS, 10 nM) for 15 min. *B.* Time course of mTORC1 (IP: Raptor) and mTORC2 (IP: Rictor) dissociation in cultured adipocytes during treatment with forskolin (FSK, 10 μM). *C.* Western blot analysis of mTORC1 and mTORC2 co-immunoprecipitations against mTOR, where cultured adipocytes were treated with or without Atglistatin (10 μM) for 1 hr prior to treatment with forskolin and insulin as in Figure 3.5*A*. *D.* Western blot analysis of mTORC2 dissociation using co-immunoprecipitations against mTOR, where WT or *Atgl* -/- primary mouse adipocytes were treated with or without insulin (10 nM) in the presence or absence of isoproterenol (0.1 μM) for 30 min as in Figures 3.1*A* and 3.1*B* before the addition of glucose. *E.* Analysis of mTORC1 dissociation *in vitro*. Recombinant mTORC1 was immunoprecipitated from HEK293T cells and the complex was incubated for 30 min with cultured 3T3-L1 adipocyte lysates from cells treated with or without forskolin (FSK, 10 μM) for 30 min prior to insulin treatment (INS, 10 nM) for 15 min. *F.* Illustrative representation of the mTOR dissociation assay. *G.* Relationship between mTOR and raptor present and Venus and Cerulean detected, respectively, as shown by western blot analysis and detection of fluorescence. *H.* mTOR dissociation assay where cultured 3T3-L1 adipocytes were treated with or without forskolin (10 μM) prior to cell lysis and lipid extraction. Purified fluorescently-tagged mTORC1 or mTORC2 was incubated with either lysate or extracted organic or aqueous phases from cultured adipocytes, or lysate from fibroblasts or hepatocytes, for 30 min prior to washing and detection of fluorescence. *I.* mTOR dissociation assay where cultured 3T3-L1 adipocytes were treated with DMSO as control, diethyl-p-

nitrophenylphosphate (E600, 150 μM), or Atglistatin (10 μM) for 1 hr prior to forskolin treatment, cell harvest, and lysate incubation with fluorescently tagged mTOR complex. *J.* mTOR dissociation assay where lipids were extracted from cultured 3T3-L1 adipocytes and treated with or without lipase *in vitro* then incubated with mTOR as in Figure 3.5*E*. Each graph represents mean ± SEM from triplicate experiments. # indicates significant difference from control ($P<0.0001$).

Figure 3.6 Torin1-Induced Inhibition of Glucose Uptake is Independent of Lipolysis.

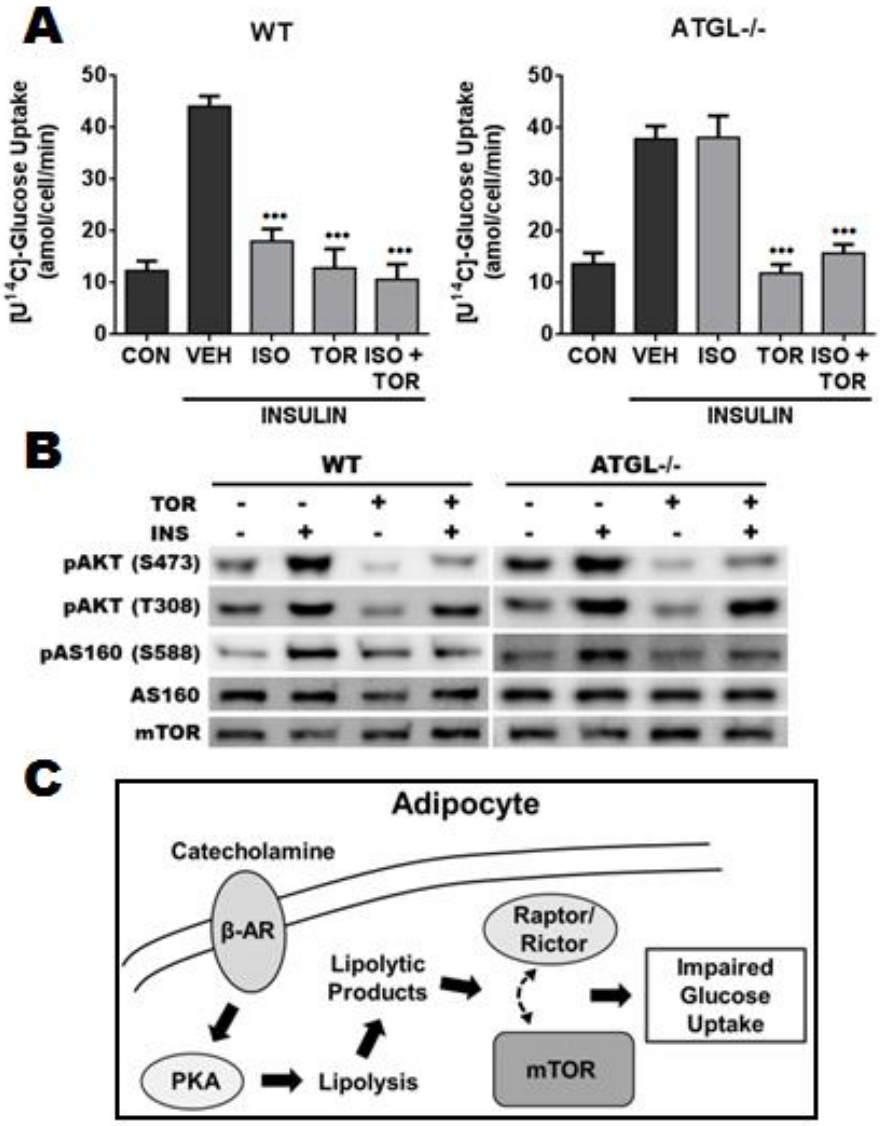

Figure 3.6 Torin1-Induced Inhibition of Glucose Uptake is Independent of Lipolysis. *A.* Radiolabeled glucose uptake assay in WT vs *Atgl* -/- primary mouse adipocytes. Isolated adipocytes were treated with or without Torin1 (250 nM) for 10 min prior to treatment with or without insulin (10 nM) in the presence or absence of isoproterenol (0.1 μM) for 30 min, followed by the addition of [U-^{14}C]-D-Glucose (10 μM) for 20 min prior to assay termination. All assays contained adenosine deaminase (ADA) (2 U/ml). *B.* Western blot analysis of insulin signaling in WT and *Atgl* -/-primary mouse adipocytes treated as in Figure 3.6*A* before the addition of glucose. *C.* Illustration of the proposed mechanism linking β-adrenergic receptor stimulation to impaired glucose uptake in adipocytes. Each graph represents mean ± SEM from triplicate experiments. Asterisk indicates significant difference ($P<0.001$ for ***).

CHAPTER 4

THE NATURE OF THE LIPOLYTIC PRODUCT(S) THAT DISSOCIATE mTOR

ABSTRACT

Adipocyte lipolytic products include traditional as well as modified forms of DAG, MAG, fatty acids, and glycerol. These products can be used as substrate for re-esterification into TAG to be stored once again in the lipid droplet, they can be exported from adipose tissue for use as energy substrates by other tissues, or they can act as signaling lipids to regulate metabolic processes. We have shown that one or more of these products inhibits insulin signaling in adipocytes by dissociating the mTOR complexes. Although the precise identity of the lipid products remains unknown, here we show our progress in the identification of these lipid(s), termed the mTOR dissociative factor. Our data suggests that the mTOR dissociative factor is an oxidized neutral lipid, most likely in fatty acid form, which is released during lipolysis. Our data also suggest that oxidized acyl chains are present in TAG and likely stored as inert lipids in the lipid droplet, released in an active form as a result of lipolysis. This has important implications in adipose tissue, as well as lipid biology. To date, there has been no known function of oxidized neutral lipids and very few examples of lipolytic products acting as signaling lipids. These results further our understanding of how both adipocyte lipolysis and oxidized neutral lipids have been overlooked as key players in metabolic regulation and potentially the pathophysiology of metabolic disease, such as insulin resistance.

INTRODUCTION

Lipolysis in adipocytes is activated by increasing cAMP concentration and subsequent PKA and lipase activity on the lipid droplet. A myriad of lipids are released from the lipid droplet during catabolic signaling and the lipids are re-esterified during anabolic signaling, such that the lipid profiles of adipocytes are in constant flux. Although activation of catabolic processes is known to inhibit anabolic signaling, the potential role of lipolytic products in regulating these cellular pathways has been underappreciated. We have shown that these lipid products of lipolysis play a significant role in regulating the crosstalk between catabolic and anabolic signaling. Here we show that some oxidized neutral lipid species released during lipolysis acts to inhibit insulin signaling by dissociating the mTOR complexes, potentially contributing to insulin resistance. To our knowledge, this is the first report of oxidized neutral lipids regulating protein function and in light of the signaling capabilities of oxidized phospholipids (90), it seems likely that oxidized neutral lipids also regulate proteins and have important cellular consequences.

Excessive caloric intake, increased mitochondrial substrate load, or mitochondrial dysfunction that amplifies the proton gradient can all increase reactive oxygen species (ROS) production (91). High levels of ROS can damage DNA and proteins, as well as produce important signaling molecules in the form of oxidized lipids. It has been established that oxidized phospholipids can be generated enzymatically or by reaction with ROS and that they play important roles in regulating protein function in both inflammation (92) and the pathogenesis of cardiovascular disease (93). Phospholipid-bound polyunsaturated fatty acids (PUFAs) are the major target for both nonenzymatic and enzymatic oxidation. Oxidative fragmentation of PUFAs results in the release of small non-esterified oxidized fatty acids such as

hydroperoxides and isoprostanes, as well as oxidation products having the complete phospholipid structure where one or both of the acyl chains contain oxidized functional groups. The mechanisms of PUFA oxidation include initiation by free radicals or nonradical ROS generated with or without enzyme activity, and through direct enzymatic oxidation by lipoxygenases (LOXs) (90). PUFAs are also commonly found esterified in neutral lipids such as TAG, DAG or MAG, and can be oxidized in a manner analogous to phospholipid-bound PUFAs. This oxidation of neutral lipids may generate several lipids that have never been examined and may have relevant physiological functions.

Intriguingly, oxidized phospholipids can cause protein complex dissociation as observed in the regulation of the transcription factor Nrf2. Under basal conditions, Nrf2 is targeted for degradation by association with Keap1, but this protein complex dissociates in the presence of specific oxidized phospholipids, resulting in Nrf2 stabilization and increased nuclear localization (90). This example of oxidized lipid-mediated protein complex dissociation results in profound physiological effects, and is very similar to the proposed oxidized neutral lipid-mediated dissociation of the mTOR complexes.

The oxidized functional groups contained in the acyl chains of oxidized phospholipids have also been shown to form covalent adducts with proteins. Oxidized phospholipids containing aldehyde or electrophilic α, β-unsaturated carbonyl groups react with nucleophilic groups such as thiols and amines, which are present in cysteine and lysine residues, respectively. This covalent modification forms Michael adducts or Schiff bases when reacting with thiols or amines, respectively, and formation of these covalent interactions has been shown to modulate the structure and/or activity of the modified proteins (90). Although this has only been observed with

oxidized phospholipids, we would expect oxidized neutral lipids to be able to regulate proteins in a similar manner.

The results described in this chapter will provide evidence for the existence of oxidized neutral lipids. We will show that numerous oxidized acyl chains are contained within TAG, and that these lipids are likely released on activation of lipolysis to generate biologically active oxidized lipids. We will provide evidence to suggest the mTOR dissociative factor is one or several of these active oxidized neutral lipids, released during lipolysis, and that its release leads to mTOR complex dissociation and inhibition. Taken together with data provided in chapter 3, these results suggest that the oxidized lipolytic products that dissociate and inhibit the mTOR complexes in adipocytes may contribute to the development of insulin resistance.

RESULTS

Oxidized Neutral Lipids. To begin to determine what lipid species is responsible for causing mTOR complex dissociation, we isolated lipids from 3T3-L1 adipocytes with or without lipolysis activated and separated these lipids using reverse-phase high-performance liquid chromatography (HPLC). The lipids were collected into separate fractions, dried, and included in *in vitro* mTORC1 kinase assays to screen for the presence of the mTOR dissociative factor **(Figure 4.1A)**. As expected, only the adipocytes undergoing lipolysis generated the mTOR dissociative factor, which was contained within fractions 5-7 **(Figure 4.1A)**. We analyzed the lipid content of each fraction using LC-MS, with a focus on detecting neutral lipids that would result from the TAG hydrolysis. Common TAGs and DAGs were eluted from the HPLC column between 8 and 10 min, and therefore mainly found within fractions 8 and 9 **(Figure 4.1B)**. Surprisingly, fractions 5-7 of the forskolin treated cell extracts were enriched in truncated neutral lipids with oxidized functional groups such as 18:0-Azelaoyl-glycerol **(Figure 4.1B)**. Reasoning that since lipolysis was required for the generation of the mTOR dissociative factor, and oxidized neutral lipids were implicated by these finding, we examined whether adipocytes accumulate oxidized lipid precursors as oxidized TAGs within the lipid droplet. We were surprised to find that 3T3-L1 adipocytes cultured under optimal conditions contain a multitude of oxidized TAGs. Several examples of oxidized TAGs were qualitatively identified in 3T3-L1 adipocyte lipid extracts by LC-MS **(Figure 4.2)**. Similar to what has been reported for oxidized phospholipids (90), we identified TAG acyl chains containing carboxylic esters, aldehydes, α, β-unsaturated aldehydes, ketones, alcohols, and carboxylic acids. These oxidized acyl chains were frequently found in TAGs with otherwise saturated acyl chains, typically 16:0-16:0, 18:0-18:0, and 16:0-18:0. The relative levels of oxidized TAGs present are still being determined, but based solely on counts per second (cps) derived peak areas our data suggest that many of the species identified

are relatively abundant. Although somewhat preliminary, this data shows that oxidized neutral lipids are fairly common in adipocytes, and lipid oxidation may play a role in the generation of the mTOR dissociative factor.

The mTOR Dissociative Factor is Likely an Oxidized Neutral Lipid. To investigate the role of lipid oxidation in generating the mTOR dissociative factor, we altered the oxidative state of adipocytes by treating with antioxidants prior to isolating the mTOR dissociative factor. Interestingly, treating adipocytes with antioxidants prior to activation of lipolysis rescued the subsequently observed mTOR complex dissociation shown both by anti-rictor co-immunoprecipitations **(Figure 4.3A)** and our mTOR dissociation assay **(Figure 4.3B)**. While antioxidant treatment likely decreased the prevalence of lipid oxidation in these adipocytes, it had no effect on levels of lipolysis as shown by glycerol release **(Figure 4.3C)**. In addition to decreasing lipid oxidation, we also treated adipocytes with the lipid soluble oxidizing agent tert-Butyl hydroperoxide (TBH), to increase lipid oxidation prior to lipolysis. After treatment, lipids were isolated and included in mTORC1 *in vitro* kinase assays to investigate their ability to dissociate the mTOR complex. Using this technique, we found that increasing concentrations of TBH prior to lipolysis generated lipids with increased ability to inhibit mTOR *in vitro* **(Figure 4.4)**. Taken together, these data suggest that the mTOR dissociative factor is likely an oxidized neutral lipid that is released during lipolysis.

Lipid Modification In Vitro. To further investigate the structure of the mTOR dissociative factor, we extracted lipids from 3T3-L1 adipocytes with or without lipolysis activated and modified these lipids *in vitro* prior to screening for the presence of the factor. Since the lipid(s) of interest are likely oxidized and may contain a carbonyl group such as a ketone or aldehyde, we reduced these groups by treatment with sodium borohydride ($NaBH_4$) prior to including these

lipids in mTOR kinase assays **(Figure 4.5)**. Reducing these carbonyl groups did not rescue mTOR activity in the presence of lipolytic products **(Figure 4.5)**, suggesting that aldehydes or ketones are not a required feature of the mTOR dissociative factor.

In addition to modifying the oxygen containing functional groups, we altered the nature of the lipids by lipid saponification. This process uses a strong base to completely hydrolyze glycerolipids into non-esterified fatty acids and free glycerol. This is useful because if the mTOR dissociative factor is a DAG or MAG, saponification should rescue mTOR complex integrity and activity, while if the factor is a fatty acid it may enhance lipid-mediated mTOR dissociation and inhibition. Surprisingly, even lipids extracted from control adipocytes were able to cause mTOR complex dissociation **(Figure 4.6A)** and inhibition **(Figure 4.6B)** after saponification, while pure fatty acids had no effect on mTOR activity **(Figure 4.6B).** Taken together, these data demonstrate that the mTOR dissociative factor is likely a fatty acid rather than a DAG or a MAG, and that it must be a specific fatty acid generated within the adipocyte rather than an effect of fatty acids in general.

DISCUSSION

Briefly discussed in chapter 3, lipotoxicity is one of the hypotheses being explored to explain the mechanisms by which obesity induces insulin resistance. Lipotoxicity is characterized by an excess in lipids that can act as signaling molecules to inhibit insulin signaling (30). The current proposed mechanism by which excess lipids, specifically DAGs, cause insulin resistance is through PKC activation. As a result, lipid-activated PKC activity is thought to decrease tyrosine phosphorylation of the insulin receptor substrate (IRS) and subsequently decrease PI3-Kinase activity and insulin signaling. Numerous studies support these findings (94-96), however many of them are based on biochemical or animal research and recent human studies have disputed the role of DAG in the development of insulin resistance (97). In addition, some human studies have shown a strong inverse association between lipids in skeletal muscle and insulin sensitivity (98, 99), but results have been inconsistent. This inverse association is not observed in conditions that promote efficient fatty acid utilization and lipid turnover, such as endurance exercise training (100). These observations have led to a paradigm known as the 'athlete paradox' where lipid accumulation does not affect insulin resistance in individuals with endurance training. Furthermore, increased lipogenesis has been shown to generate branched-chain fatty acids that protect against insulin resistance, implicating that some lipid structures may improve glucose tolerance (101). This is interesting because it highlights that different lipids can impact glucose homeostasis in opposite ways, suggesting that lipotoxicity, or toxic levels of overall lipids, may be irrelevant in the development of lipid-mediated insulin resistance, and investigating the types of lipids present may be more useful. In addition to lipotoxicity, oxidative stress has been implicated in the development of insulin resistance.

Oxidative stress is considered in 'steady state' when the ROS flux is balanced by antioxidant defenses. An increase of oxidative stress, which occurs in conditions of augmented ROS and/or reduction in antioxidant levels, has been shown to play a critical role in the development of obesity-induced insulin resistance through adipocyte dysfunction (102-105). In addition, oxidative stress is increased in obese individuals (106), and is thought to contribute to the development of obesity-induced insulin resistance. However, like lipid-induced insulin resistance, the evidence is inconsistent and the mechanism linking oxidative damage to insulin resistance in adipose tissue remains largely unknown.

We hypothesize that lipids, specifically fatty acids, do contribute to insulin resistance in adipose tissue, but only when oxidized. This finding will potentially reconcile the inconsistent results in finding lipid-induced insulin resistance, and explain the 'athlete paradox' in that high lipid turnover will decrease overall lipid oxidation due to less storage time, causing tissues to remain sensitive to insulin. As previously mentioned, while both lipid concentration and oxidative stress have been implicated in the progression of insulin resistance in obesity, data has not been consistent in either case. We believe that it is the generation of oxidized lipids that directly inhibit insulin-stimulated glucose uptake rather than independent effects of lipids or ROS alone **(Figure 4.7)**. We also show evidence that the oxidized lipid's mechanism of action is direct inhibition of the mTOR complexes, leading to decreased insulin-stimulated glucose uptake.

Adipocytes store vast quantities of lipids in the form of TAG in the lipid droplet and we have found that even under non-pathological conditions there is a considerable quantity of oxidized acyl chains esterified into TAG. Our findings suggest that this previously unrecognized component of the lipid droplet, although stored in inert form as TAG, may be converted into the

mTOR dissociative factor during lipolysis, which is responsible for attenuated insulin signaling. However, our results do not rule out that the dissociative factor may be oxidized after lipids containing unsaturated acyl chains are released from the lipid droplet. Therefore, more work is required to confirm this hypothesis.

Another question that remains regarding the mTOR dissociative factor is: how does it cause mTOR complex dissociation? Although more work is required to fully investigate this, we propose that the lipid(s) causing mTOR complex dissociation may be competing with phosphatidic acid (PA) to bind mTOR. PA is generated by phospholipase D activity as well as other enzymes and is an intermediate lipid in fatty acid esterification into TAG. PA has been demonstrated to bind directly to the Rapamycin-FKBP12 Binding (FRB) domain of mTOR and to positively regulate its activity (53, 59, 107). It is speculated that PA activates mTOR through strengthening the association between proteins within the complex, and that the mTOR complexes may dissociate in the absence of PA. We hypothesize that the mTOR dissociative factor may also bind the FRB domain, preventing mTOR activation and stabilization by PA.

Current Assessment of the mTOR Dissociative Factor. Although questions still remain, this preliminary work provides compelling evidence of the existence and specific nature of a lipid intermediate that inhibits the mTOR complexes. Taking relevant data from chapters 3 and 4 into account, here is what we can currently conclude about the nature of the mTOR dissociative factor:

- The dissociative factor is produced during lipolysis in adipocytes and inhibiting lipolysis eliminates its activity on the mTOR complexes **(Figures 3.3B, 3.3C, 3.4C, 3.5C, 3.5D, and 3.5I)**.

- The dissociative factor partitions to the organic fraction, is transferrable *in vitro*, and can be partially isolated by reverse-phase HPLC, suggesting it is a hydrophobic molecule, likely a glycerolipid **(Figures 3.4B, 3.5E, 3.5H, and 4.1A)**.
- The dissociative factor can be generated by the breakdown of lipids extracted from adipocytes *in vitro* by lipase treatment or saponification, and pure fatty acids have no effect on mTOR activity *in vitro*, suggesting it is likely a specific fatty acid that is generated during lipolysis. **(Figures 3.4D, 3.4E, 3.5J, 4.6A, and 4.6B)**
- The dissociative factor is likely an oxidized fatty acid, as indicated by manipulation of lipid oxidation by treatment with antioxidants or oxidizing agents, which decrease or increase the production of the dissociative factor, respectively **(Figures 4.3A, 4.3B, and 4.4)**.
- Neither aldehydes nor ketones are required functional groups within the structure of the dissociative factor **(Figure 4.5)**.

Figure 4.1 Reverse-Phase HPLC to Isolate the mTOR Dissociative Factor.

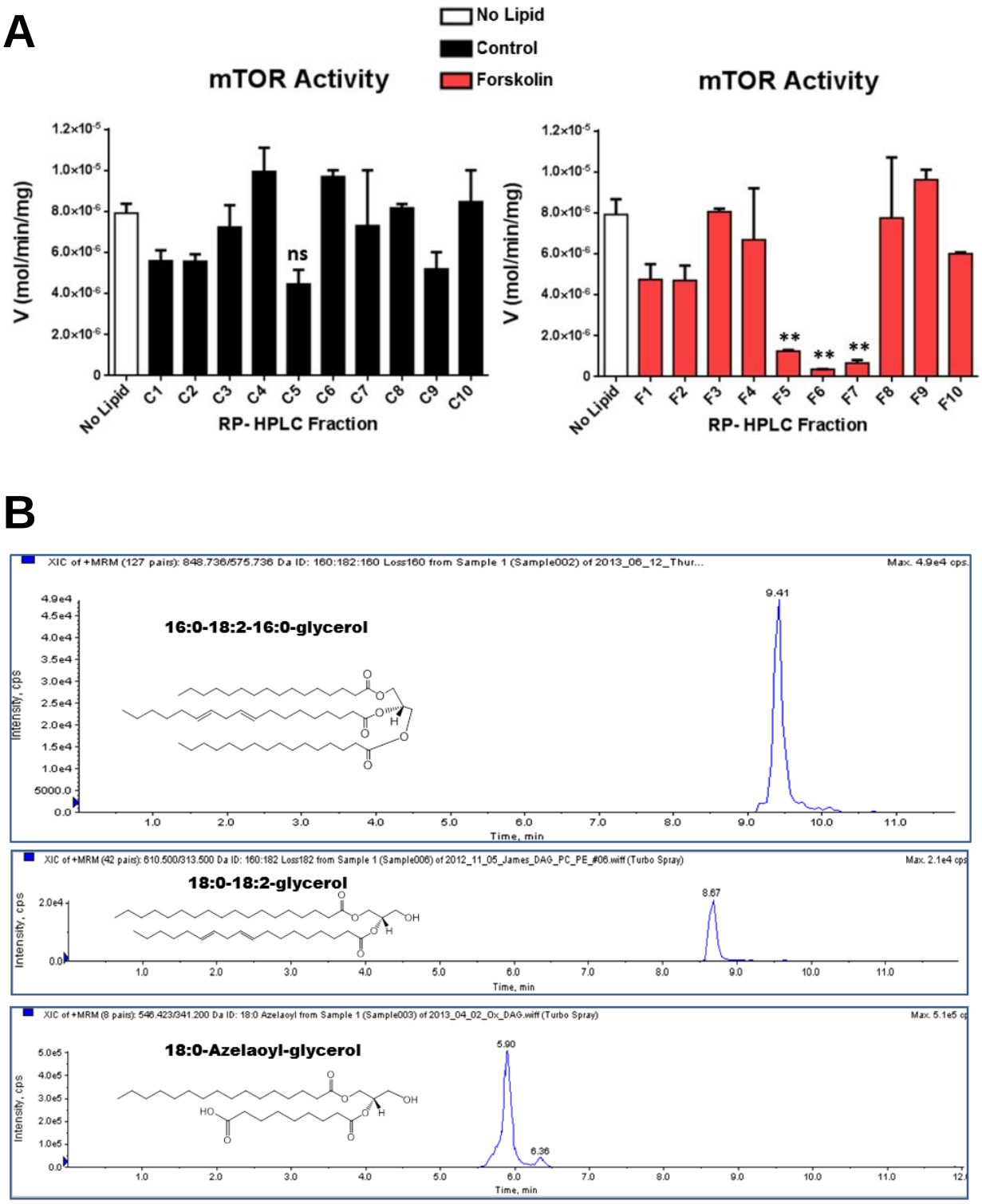

Figure 4.1 Reverse-Phase HPLC to Isolate the mTOR Dissociative Factor. *A.* Lipids from either control or forskolin treated 3T3-L1 adipocytes were extracted using 1:1; hexane: ethyl acetate and separated by C18 reverse-phase HPLC. Fractions were collected at one minute intervals. The amount of extract from 0.02 of 6 cm plates were collected from each fraction, dried, and included in an *in vitro* mTORC1 kinase assay as in Figures 3.4*B*-*E.* Each graph represents mean ± SEM from duplicate experiments. Asterisk indicates significant difference ($P<0.01$ for **). *B.* Chromatograms showing retention times of 16:0-18:2-16:0-glycerol (TAG), 18:0-18:2-glycerol (DAG), and 18:0- azelaoyl-glycerol (oxidized DAG) from lipids extracted from 3T3-L1 adipocytes. Each minute directly corresponds with the fractions used in Figure 4.1*A.* The structures of 16:0-18:2-16:0-glycerol and 18:0-18:2-glycerol are depicted in the trans conformation rather than the correct cis conformation due to space limitations.

Figure 4.2 Oxidized Triacylglycerol Identified in 3T3-L1 Adipocytes.

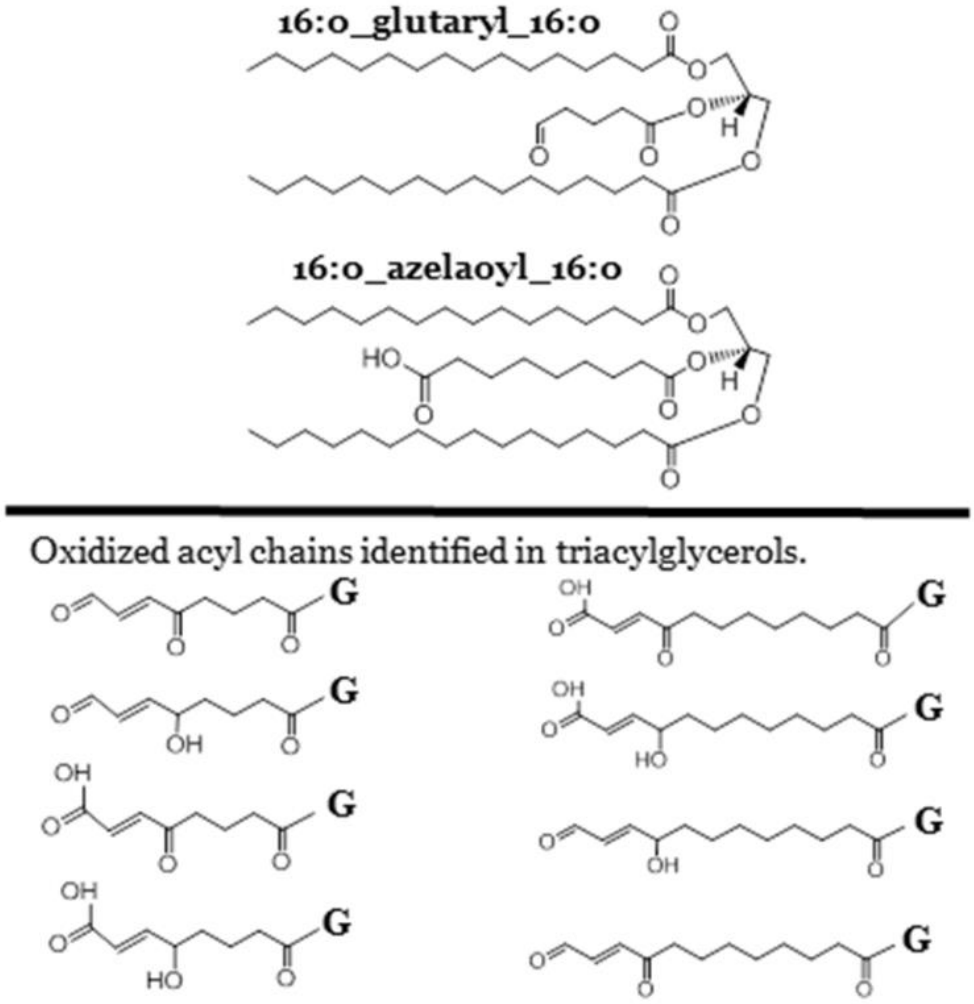

Figure 4.2 Oxidized Triacylglycerol Identified in 3T3-L1 Adipocytes. Structures of the types of oxidized triacylglycerol found by LC-MS in 3T3-L1 adipocytes, where G indicates glycerol attachment. Categorical identification is still tentative and based solely on neutral loss of predicted masses of acyl chains from all three positions on the glycerol backbone.

Figure 4.3 Antioxidants Rescue mTOR Complex Dissociation.

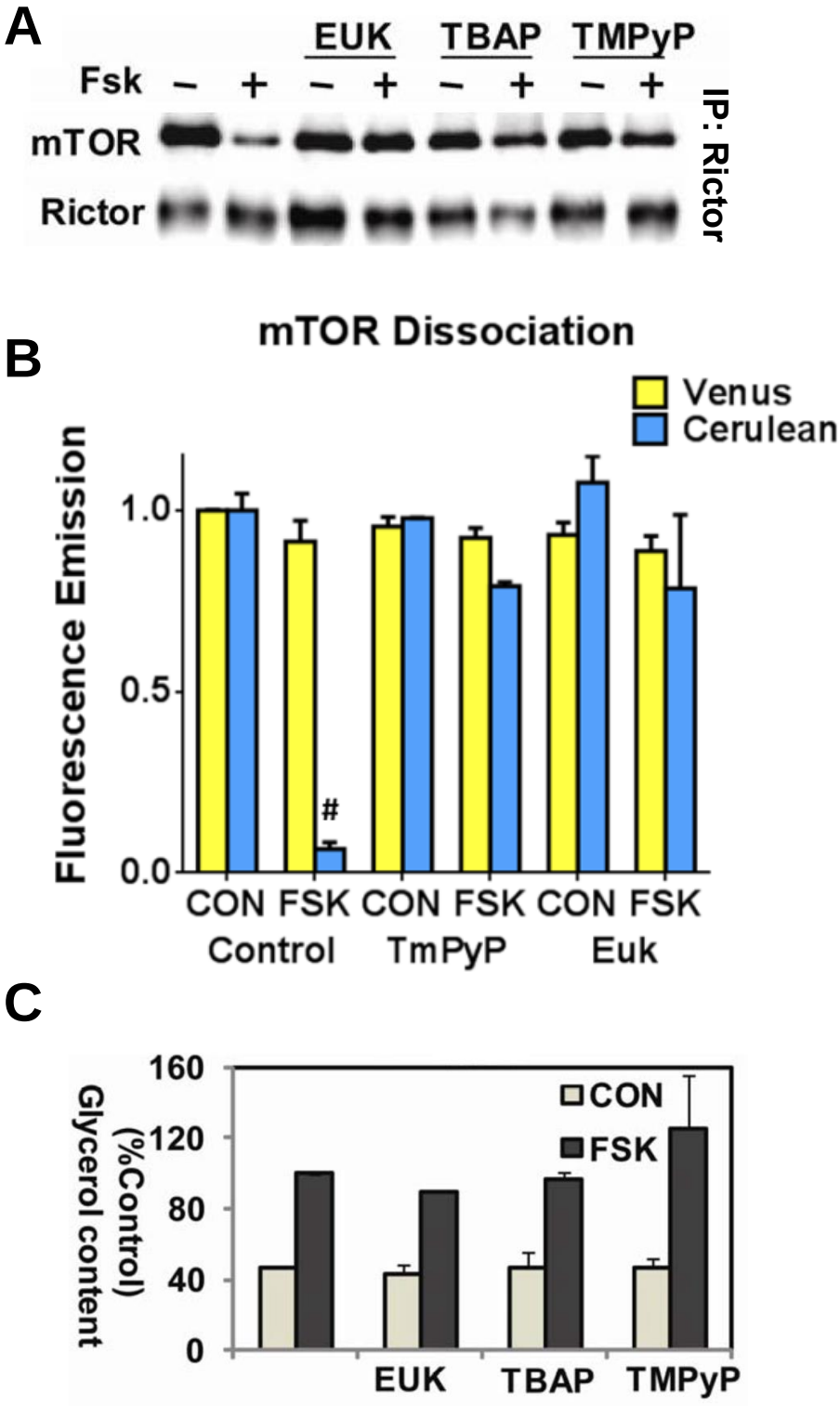

Figure 4.3 Antioxidants Rescue mTOR Complex Dissociation. *A.* Anti-Rictor Immunoprecipitations of 3T3-L1 adipocyte lysates. Adipocytes were either treated with vehicle or the antioxidants EUK, TBAP, or TMPyP for 24 hrs before treatment with or without forskolin (10 μM) for 30 min prior to cell harvest, immunoprecipitation against rictor, and immunoblotting for mTOR and rictor to assess mTORC2 complex dissociation. *B.* mTOR dissociation assays done as in Figures 3.*5G-J* using lipids extracted from 3T3-L1 adipocytes treated as in Figure 4.3*A*, where EUK and TMPyP were used as antioxidants. Graph represents mean ± SEM from triplicate experiments. # indicates significant difference from control ($P<0.0001$). *C.* Glycerol released from 3T3-L1 adipocytes treated as in Figure 4.*3A* was measured to control for changes in lipolysis as a result of treatment with antioxidants. Graph represents mean ± SEM from duplicate experiments.

Figure 4.4 Lipid Oxidation Further Inhibits mTORC1 Activity *In Vitro*.

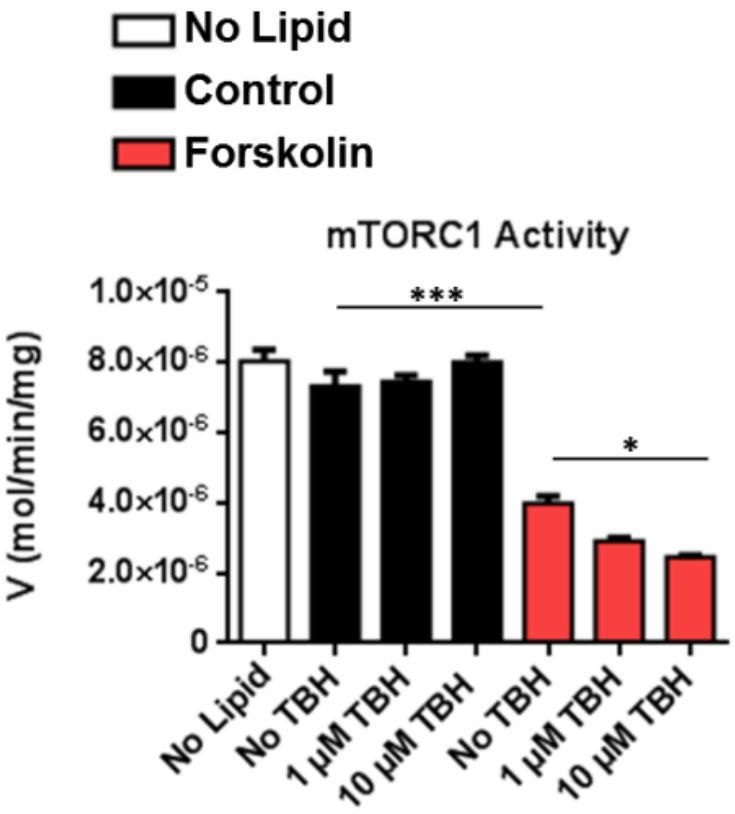

Figure 4.4 Lipid Oxidation Further Inhibits mTORC1 Activity *In Vitro*. *In vitro* mTORC1 kinase assays where lipids extracted from 3T3-L1 adipocytes were added to assess mTOR inhibition. Adipocytes were treated with or without tert-Butyl hydroperoxide (TBH), a lipid soluble oxidizing agent, at the indicated concentrations for 2 hrs prior to treatment with or without forskolin (10 μM) for 30 min. Cells were harvested and lipids were extracted using 1:1; hexane: ethyl acetate and dried before re-suspension in kinase assay buffer and addition to the kinase assays. Graph represents mean ± SEM from duplicate experiments. Asterisk indicates significant difference ($P<0.05$ or $P<0.001$ for *, *** respectively).

Figure 4.5 Lipid Reduction by Sodium Borohydride Does Not Rescue mTOR Activity.

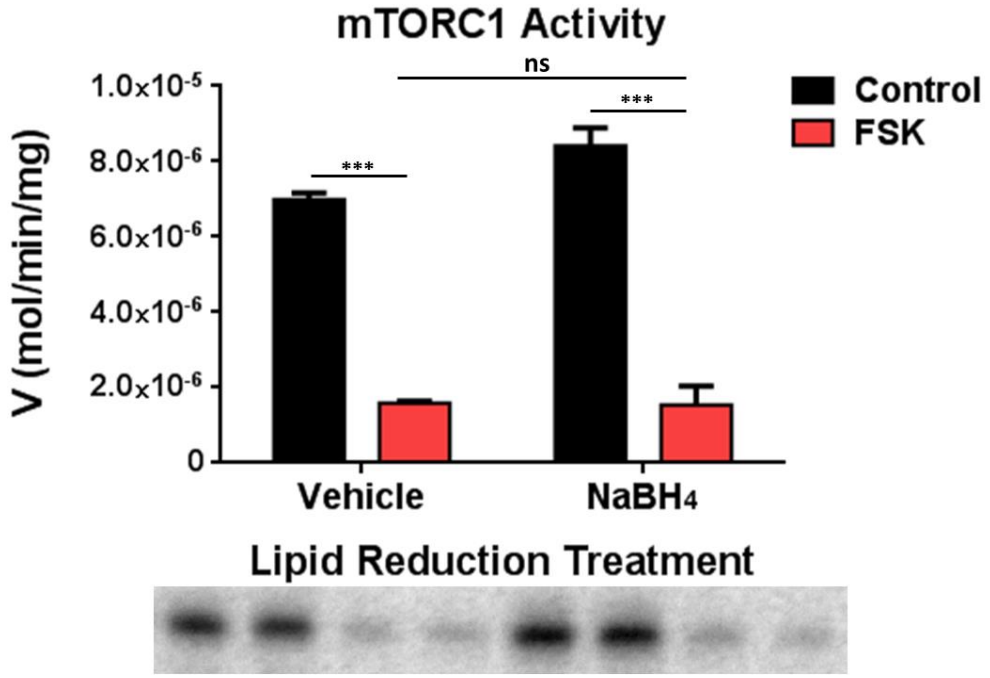

Figure 4.5 Lipid Reduction by Sodium Borohydride Does Not Rescue mTOR Activity. *In vitro* mTOR kinase assay using lipids extracted from 3T3-L1 adipocytes treated with or without forskolin (10 μM) for 45 min prior to cell harvest and lipid extraction. Dried lipids were re-suspended in buffer A with or without the reducing agent sodium borohydride ($NaBH_4$, 2mM) and incubated for 15 min at room temperature to reduce carbonyl groups such as aldehydes and ketones. Lipids were then re-extracted, dried, re-suspended in kinase buffer and included in mTOR kinase assays. Graph represents mean ± SEM from duplicate experiments. Asterisk indicates significant difference ($P<0.001$ for ***). Lower panel is the radiograph generated by P-32 labeled 4E-BP1, the mTORC1 substrate used in the kinase assay.

Figure 4.6 Saponified Lipids from Adipocytes Cause mTOR Complex Dissociation.

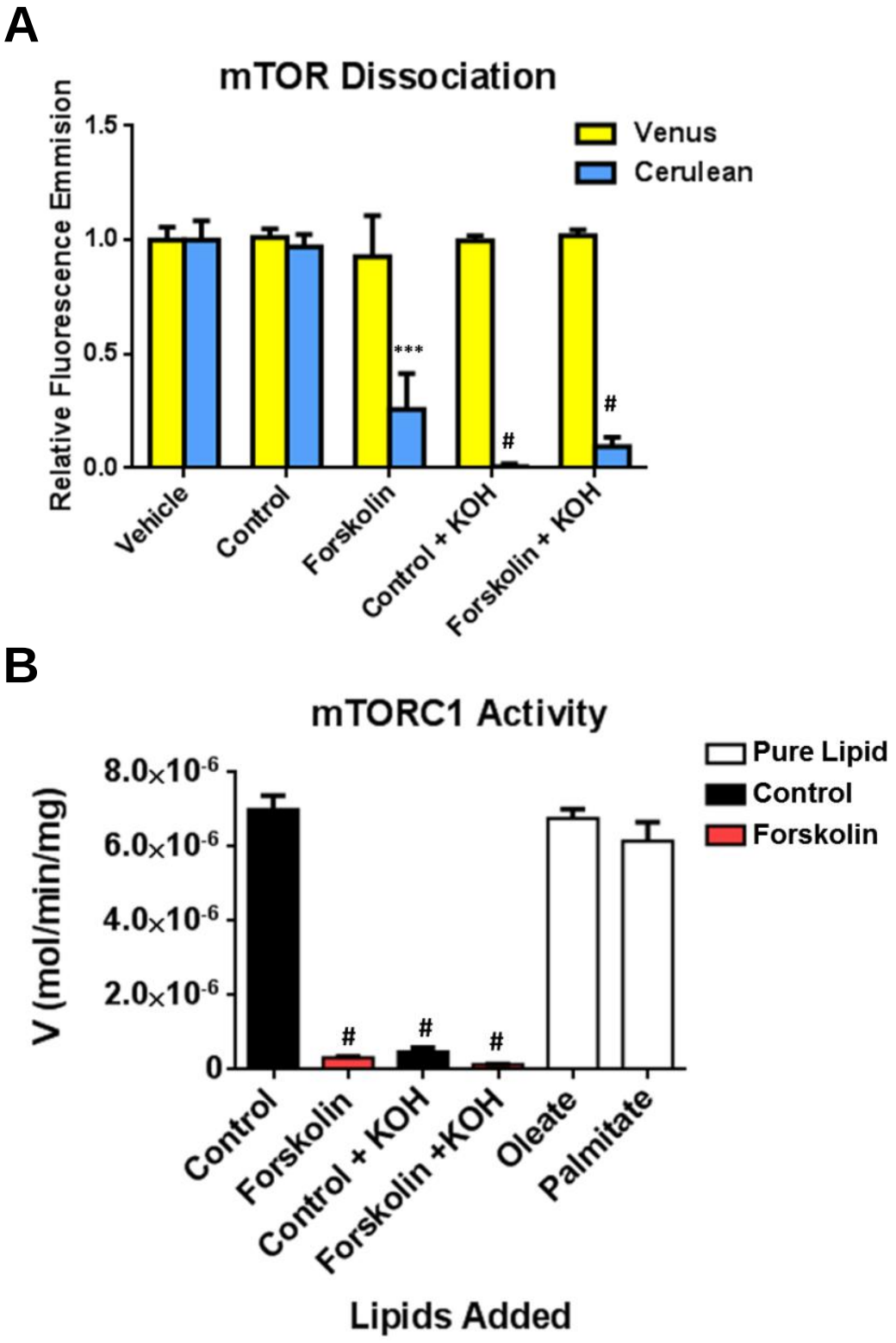

Figure 4.6 Saponified Lipids from Adipocytes Cause mTOR Complex Dissociation. *A.* mTOR dissociation assay using lipids extracted from 3T3-L1 adipocytes. Cells were treated with or without forskolin (10 μM) for 45 min prior to harvest and lipid extraction. Lipids were then dried and treated with or without 200 mM potassium hydroxide (KOH) at 30 °C for 30 min prior to re-extraction and addition into the mTOR dissociation assay. Vehicle buffer was treated with KOH parallel to KOH treated lipids. Graph represents mean ± SEM from triplicate experiments. Asterisk or # indicate significant difference from control ($P<0.001$ or $P<0.0001$ for *** and #, respectively). *B. In vitro* mTOR kinase assays using lipids extracted from 3T3-L1 adipocytes and treated as in Figure 4.5*A*, or using pure oleate or palmitate (10 μM) to assess mTOR inhibition by these pure lipids. Graph represents mean ± SEM from duplicate experiments. # indicate significant difference from control ($P<0.0001$).

Figure 4.7 Proposed Mechanistic Links Between Obesity-, Stress-, Lipid-, and ROS-Induced Insulin Resistance.

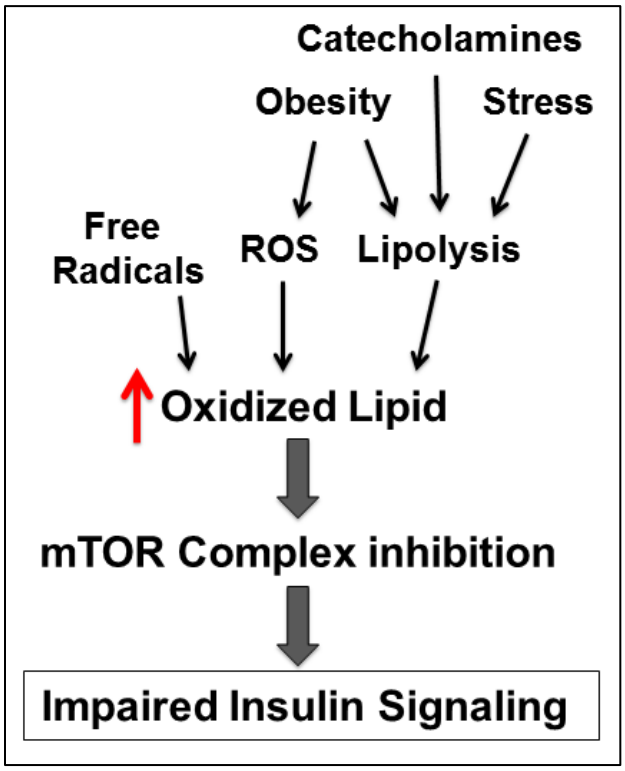

Figure 4.7 Proposed Mechanistic Links Between Obesity-, Stress-, Lipid-, and ROS-Induced Insulin Resistance. The finding that oxidized neutral lipids inhibit the mTOR complexes provides a mechanistic link between Obesity-, Stress-, Lipid-, and ROS-Induced Insulin Resistance. Obesity, stress, and catecholamine action lead to elevated levels of lipolysis, causing an increase in lipid accumulation. Free radicals and ROS contribute to lipid oxidation, generating oxidized lipid intermediates that we propose directly inhibit the mTOR complexes, leading to insulin resistance.

CHAPTER 5

CONCLUSIONS, MEDICAL SIGNIFICANCE, AND FUTURE DIRECTIONS

Conclusions

These studies reveal the molecular mechanism of catecholamine-mediated inhibition of glucose uptake in adipocytes. Catecholamines activate lipolysis through β-adrenergic stimulation, which leads to the release of an oxidized lipid product that dissociates the mTOR complexes and subsequently inhibits insulin signaling to decrease glucose uptake **(Figure 5.1)**. In a multidisciplinary approach, we have used genetic, pharmacological, and biochemical methods to discover this unique mechanism of opposition between catabolic processes and anabolic signaling. This is a novel mechanism of mTOR regulation that leads to insulin resistance and may have medical relevance with respect to the development of obesity-induced insulin resistance and stress-induced hyperglycemia. Accordingly, this research likely lays the groundwork for further research leading to therapeutic treatments that improve patient care and survival during the development of these conditions.

Summary of Scientific Contributions

We provide compelling evidence that catecholamine-mediated adipocyte lipolysis releases a lipid intermediate, likely an oxidized lipid that dissociates the mTOR complexes and subsequently inhibits insulin-stimulated glucose uptake **(Figure 5.1)**. This novel mechanism of opposition between catabolic and anabolic pathways has significantly advanced the studies of adipocyte insulin signaling, lipolysis, and mTOR regulation in several ways. First, this mechanism is the unknown pathway whereby insulin-stimulated glucose uptake is inhibited by

catecholamines. Second, it provides new insight into the mechanisms of opposition between anabolic and catabolic signaling in adipocytes. Third, this mechanism provides new, reconciling evidence for the role of lipids and oxidation in the development of insulin resistance. Fourth, it highlights the importance of lipolysis in regulating cellular signaling events, as a potential consequence of releasing energy stores. Fifth, it suggests that oxidized lipids are lipolytic products that can act as signaling molecules with physiological relevance. Sixth, this mechanism introduces a novel pathway of mTOR regulation in adipocytes. Seventh, it provides a possible link between obesity and the development of insulin resistance. And finally, it provides a likely mechanism for how the stress response leads to acute insulin resistance and hyperglycemia. In addition, while the structural identification of the mTOR dissociative factor is ongoing, the structure of this lipid will lay the groundwork for developing novel compounds with unique effects on mTORC1 and 2. Given the importance of mTOR signaling in human disease, this has potential to greatly advance new therapeutic strategies involving the mTOR complexes.

Medical Significance

Stress-Induced Hyperglycemia. As previously discussed, stress-induced hyperglycemia develops after trauma or major surgery, particularly surgery within the abdominal cavity (33), after severe burn injuries, or sepsis. If untreated it contributes to mortality and delays healing in post-surgery and ICU patients (34). As a result, blood glucose monitoring and subsequent insulin therapy is common practice during recovery from surgery or during severe illness in the ICU. Activation of the adaptive stress response results in the release of catabolic agents that will activate lipolysis; including catecholamines, cortisol, growth factors, and inflammatory cytokines. Furthermore, it has been shown that adipose tissue becomes resistant to insulin prior to skeletal muscle and liver

during the stress response (47), suggesting it may play a role in the initial development of stress-induced hyperglycemia. Our work establishes that catecholamine-mediated lipolysis leads to insulin resistance in adipocytes. Taken together, these findings strongly implicate our proposed mechanism in the development of stress-induced hyperglycemia. Understanding this possible mechanism of stress-induced insulin resistance could lay the groundwork for future therapeutic treatments to improve patient outcomes after surgery. In addition, monitoring levels of lipolysis may prove useful in predicting risk of hyperglycemia after trauma or major surgery.

Obesity-induced insulin resistance. In 2010, it was estimated that 68% of the population could be defined as overweight and greater than 30% as obese (108). Over-nutrition and sedentary lifestyles largely contribute to this weight gain, the resulting health problems, and rising health-care costs each year. Along with other health issues, type 2 diabetes is frequently concurrent with obesity (109), but the mechanistic basis for obesity-induced insulin resistance remains largely unknown. Abdominal obesity is accompanied by a chronic, low-grade inflammation. In obese humans, while catecholamine stimulation of lipolysis is sometimes dampened, basal levels of lipolysis are commonly elevated (9), and high levels of circulating lipolytic products often correlate with obesity and insulin resistance in type 2 diabetes (30, 110). Furthermore, insulin resistance is often associated with lipid accumulation in liver and skeletal muscle (32, 85), and impaired lipolysis due to lipase deficiency in mice attenuates diet-induced insulin resistance (27, 28). Concurrent with these findings, our work suggests that in addition to the acute events investigated within this report, it is possible that adipocyte lipolysis and subsequent inhibition of the mTOR signaling pathway plays a role in the development of insulin resistance that occurs during obesity. It is likely that many factors including inflammatory cytokines (111) and increased sympathetic tone (112, 113) contribute to this increase in lipolysis,

which may play a role in the development of insulin resistance. In addition, oxidative stress is increased in obese individuals and in adipose tissue from genetically obese mice (106), and increased ROS has been implicated in the development of diet-induced insulin resistance (104, 105), suggesting that lipid oxidation may be more prevalent during obesity as well.

Although further investigation is necessary to determine the contribution of lipolytic-mediated inhibition of the mTOR complexes to obesity-induced insulin resistance in adipose tissue, our finding that oxidized lipid metabolites produced during lipolysis antagonize insulin signaling represents significant progress in understanding the mechanisms that contribute and may pave the way for the development of new treatment approaches.

Future Directions

This work began with the goal of determining the molecular mechanism of catecholamine-mediated inhibition of glucose uptake in adipocytes. Future studies should include several areas of research, including identifying the specific structure of the mTOR dissociative factor, investigating the possible role of this novel pathway in the development of both stress-induced hyperglycemia and obesity-induced insulin resistance, and investigating other possible physiological roles of oxidized neutral lipids.

Identifying the structure of the mTOR dissociative factor can be examined on multiple fronts. High-performance liquid chromatography can continue to be used in conjunction with mTOR kinase assays and detection of lipids by mass spectrometry to investigate the lipid class of the dissociative factor. The results can inform efforts to derivatize isolated lipids using reagents such as pentafluorobenzyl or methoxyamine (114) to identify essential functional groups. Another approach is to oxidize known pure lipids *in vitro* in an attempt to generate the oxidized lipid that will dissociate the mTOR complexes. And finally, to confirm the structure, the mTOR

dissociative factor candidates could be synthesized and tested on mTOR *in vitro*. Identifying the structure of this lipid will give novel insight into one of the mechanisms of mTOR regulation, and will pave the way for new therapeutic compounds that target the mTOR complexes.

To investigate the role that lipolysis-mediated inhibition of mTOR may play in stress-induced hyperglycemia, a mouse model for abdominal surgery could be used. It has been demonstrated that this model leads to hyperglycemia in mice (35, 36, 47, 115, 116), and we propose that genetic or pharmacological inhibition of lipolysis during surgery may rescue blood glucose. mTOR complex dissociation and insulin signaling in adipose tissue during recovery from surgery should also be assessed.

Genetic and pharmacological inhibition of lipolysis during diet-induced obesity will also be useful in determining the role of our proposed mechanism in the development of obesity-induced insulin resistance. Along with adipocyte glucose uptake and whole body glucose homeostasis, insulin signaling and mTOR complex integrity can be rigorously investigated in this model.

The discovery that oxidized neutral lipids are released during lipolysis and have a role in regulating adipocyte function has provided fertile ground for future investigation of these lipids and their biological relevance. The first step to examining these lipids is to develop qualitative and quantitative detection methods. Lipids produced during lipolysis are typically exported from adipose tissue into circulation for use by other tissues. Mass spectrometry analysis of these lipids in blood and other tissues would provide evidence that they are released from adipose tissue, and may regulate other cellular processes. Accordingly, it would be interesting to pursue these lipids as potential biomarkers for risk of insulin resistance or the progression of type 2 diabetes.

Figure 5.1 Proposed Mechanism of Catecholamine-Induced Decrease in Glucose Uptake in Adipocytes.

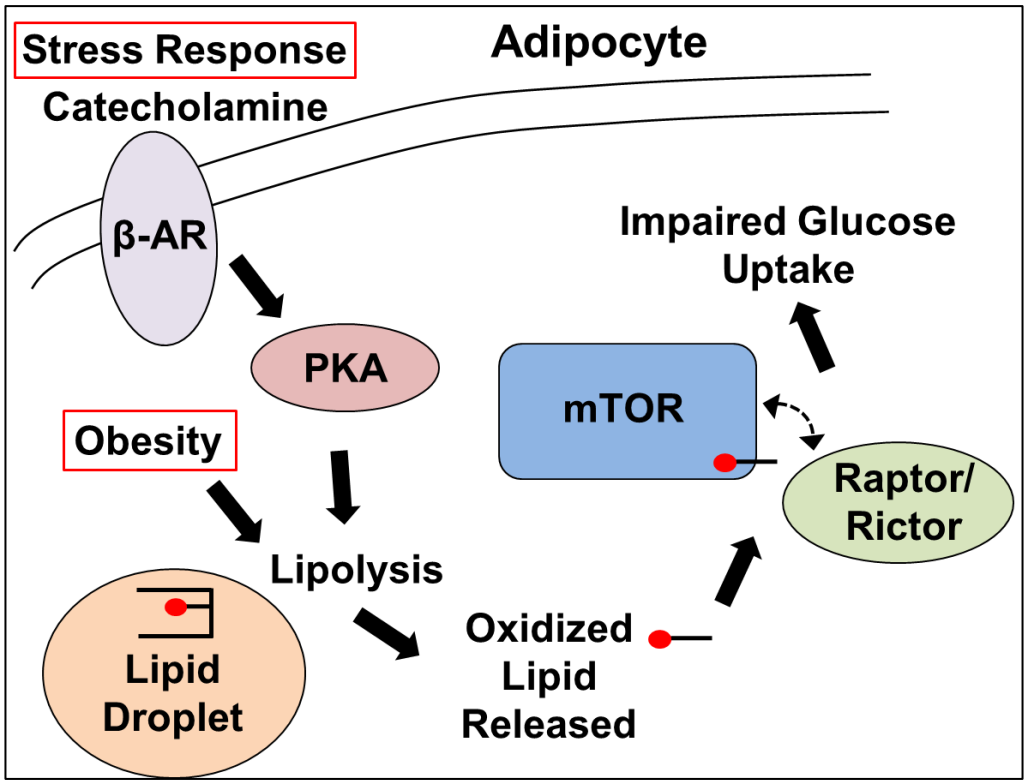

Figure 5.1 Proposed Mechanism of Catecholamine-Induced Decrease in Glucose Uptake in Adipocytes. β-adrenergic stimulation by catecholamines leads to activation of PKA and subsequent activation of lipolysis. Hydrolysis of stored TAG in the lipid droplet releases a lipid intermediate, likely an oxidized fatty acid that dissociates the mTOR complexes, resulting in impaired glucose uptake in response to insulin.

CHAPTER 6

PUBLICATIONS RESULTING FROM THIS WORK

Mullins, G.R., Wang, L., Sherwood, S.G., Eaton, J.M., Boroda, S., Blancquaert, S., Roger, P.P., Leitinger, N., Harris, T.E. 2014. Catecholamine-Induced Lipolysis Inhibits Glucose Uptake and Causes mTOR Complex Dissociation in Adipocytes. *Proceedings of the National Academy of Sciences* 111, 17450-5.

Mullins, G.R., Wang, L., Harris, T.E. 2014. Lipolysis Suppresses Insulin Signaling and Glucose Uptake [Abstract]. *Clinical Chemistry* 60, S274. Abstract B-387.

ADDITIONAL PUBLICATIONS

Eaton, J.M., Takkellapati, S., Lawrence, R.T., McQueeney, K.E., Boroda, S., **Mullins, G.R.**, Sherwood, S.G., Finck, B.N., Villén, J., and Harris, T.E. 2014. Lipin 2 Binds Phosphatidic Acid by the Electrostatic-Hydrogen Bond Switch Mechanism Independent of Phosphorylation. *The Journal of Biological Chemistry* 289, 18055-66.

Dominguez, C.L., Floyd, D.H., Xiao, A., **Mullins, G.R.**, Kefas, B.A., Xin, W., Yacur, M.N., Abounader, R., Lee, J.K., Mustata Wilson, G., Harris, T.E., and Purow, B.W. 2013. Diacylglycerol kinase alpha is a critical signaling node and novel therapeutic target in glioblastoma and other cancers. *Cancer Discovery* 3, 782-97.

Eaton, J.M., **Mullins, G.R.**, Brindley, D.N., and Harris, T.E. 2013. Phosphorylation of lipin 1 and charge on the phosphatidic Acid head group control its phosphatidic Acid phosphatase activity and membrane association. *The Journal of Biological Chemistry* 288, 9933-45.

REFERENCES

1. Holm C (2003) Molecular mechanisms regulating hormone-sensitive lipase and lipolysis. *Biochem Soc Trans*, pp 1120-1124.
2. Miyoshi H, Souza SC, Zhang HH, Strissel KJ, Christoffolete MA, Kovsan J, Rudich A, Kraemer FB, Bianco AC, Obin MS, & Greenberg AS (2006) Perilipin promotes hormone-sensitive lipase-mediated adipocyte lipolysis via phosphorylation-dependent and -independent mechanisms. *J Biol Chem* 281(23):15837-15844.
3. Brasaemle DL, Subramanian V, Garcia A, Marcinkiewicz A, & Rothenberg A (2009) Perilipin A and the control of triacylglycerol metabolism. *Mol Cell Biochem* 326(1-2):15-21.
4. Zimmermann R, Lass A, Haemmerle G, & Zechner R (2009) Fate of fat: the role of adipose triglyceride lipase in lipolysis. *Biochim Biophys Acta* 1791(6):494-500.
5. Subramanian V, Rothenberg A, Gomez C, Cohen AW, Garcia A, Bhattacharyya S, Shapiro L, Dolios G, Wang R, Lisanti MP, & Brasaemle DL (2004) Perilipin A mediates the reversible binding of CGI-58 to lipid droplets in 3T3-L1 adipocytes. *J Biol Chem* 279(40):42062-42071.
6. Egan JJ, Greenberg AS, Chang MK, Wek SA, Moos MC, Jr., & Londos C (1992) Mechanism of hormone-stimulated lipolysis in adipocytes: translocation of hormone-sensitive lipase to the lipid storage droplet. *Proc Natl Acad Sci U S A* 89(18):8537-8541.
7. Anthonsen MW, Ronnstrand L, Wernstedt C, Degerman E, & Holm C (1998) Identification of novel phosphorylation sites in hormone-sensitive lipase that are phosphorylated in response to isoproterenol and govern activation properties in vitro. *J Biol Chem* 273(1):215-221.
8. Chaves VE, Frasson D, & Kawashita NH (2011) Several agents and pathways regulate lipolysis in adipocytes. *Biochimie* 93(10):1631-1640.
9. Duncan RE, Ahmadian M, Jaworski K, Sarkadi-Nagy E, & Sul HS (2007) Regulation of lipolysis in adipocytes. *Annu Rev Nutr* 27:79-101.
10. Zechner R, Zimmermann R, Eichmann TO, Kohlwein SD, Haemmerle G, Lass A, & Madeo F (2012) FAT SIGNALS--lipases and lipolysis in lipid metabolism and signaling. *Cell Metab* 15(3):279-291.
11. Summers SA, Whiteman EL, & Birnbaum MJ (2000) Insulin signaling in the adipocyte. *Int J Obes Relat Metab Disord* 24 Suppl 4:S67-70.
12. Berggreen C, Gormand A, Omar B, Degerman E, & Goransson O (2009) Protein kinase B activity is required for the effects of insulin on lipid metabolism in adipocytes. *Am J Physiol Endocrinol Metab* 296(4):E635-646.
13. Wijkander J, Landstrom TR, Manganiello V, Belfrage P, & Degerman E (1998) Insulin-induced phosphorylation and activation of phosphodiesterase 3B in rat adipocytes: possible role for protein kinase B but not mitogen-activated protein kinase or p70 S6 kinase. *Endocrinology* 139(1):219-227.
14. Green A (1983) Catecholamines inhibit insulin-stimulated glucose transport in adipocytes, in the presence of adenosine deaminase. *FEBS Lett* 152(2):261-264.
15. Carpene C, Chalaux E, Lizarbe M, Estrada A, Mora C, Palacin M, Zorzano A, Lafontan M, & Testar X (1993) Beta 3-adrenergic receptors are responsible for the adrenergic inhibition of insulin-stimulated glucose transport in rat adipocytes. *Biochem J* 296 (Pt 1):99-105.
16. Deibert DC & DeFronzo RA (1980) Epinephrine-induced insulin resistance in man. *J Clin Invest* 65(3):717-721.
17. Smith U, Kuroda M, & Simpson IA (1984) Counter-regulation of insulin-stimulated glucose transport by catecholamines in the isolated rat adipose cell. *J Biol Chem* 259(14):8758-8763.
18. Kuroda M, Honnor RC, Cushman SW, Londos C, & Simpson IA (1987) Regulation of insulin-stimulated glucose transport in the isolated rat adipocyte. cAMP-independent effects of lipolytic and antilipolytic agents. *J Biol Chem* 262(1):245-253.

19. Joost HG, Habberfield AD, Simpson IA, Laurenza A, & Seamon KB (1988) Activation of adenylate cyclase and inhibition of glucose transport in rat adipocytes by forskolin analogues: structural determinants for distinct sites of action. *Mol Pharmacol* 33(4):449-453.
20. Van Obberghen E, Baron V, Delahaye L, Emanuelli B, Filippa N, Giorgetti-Peraldi S, Lebrun P, Mothe-Satney I, Peraldi P, Rocchi S, Sawka-Verhelle D, Tartare-Deckert S, & Giudicelli J (2001) Surfing the insulin signaling web. *Eur J Clin Invest* 31(11):966-977.
21. Lizcano JM & Alessi DR (2002) The insulin signalling pathway. *Curr Biol* 12(7):R236-238.
22. Taniguchi CM, Emanuelli B, & Kahn CR (2006) Critical nodes in signalling pathways: insights into insulin action. *Nat Rev Mol Cell Biol* 7(2):85-96.
23. Gan X, Wang J, Su B, & Wu D (2011) Evidence for direct activation of mTORC2 kinase activity by phosphatidylinositol 3,4,5-trisphosphate. *J Biol Chem* 286(13):10998-11002.
24. Manning BD & Cantley LC (2007) AKT/PKB signaling: navigating downstream. *Cell* 129(7):1261-1274.
25. Minokoshi Y, Kahn CR, & Kahn BB (2003) Tissue-specific ablation of the GLUT4 glucose transporter or the insulin receptor challenges assumptions about insulin action and glucose homeostasis. *J Biol Chem* 278(36):33609-33612.
26. Kumar A, Lawrence JC, Jr., Jung DY, Ko HJ, Keller SR, Kim JK, Magnuson MA, & Harris TE (2010) Fat cell-specific ablation of rictor in mice impairs insulin-regulated fat cell and whole-body glucose and lipid metabolism. *Diabetes* 59(6):1397-1406.
27. Hoy AJ, Bruce CR, Turpin SM, Morris AJ, Febbraio MA, & Watt MJ (2011) Adipose triglyceride lipase-null mice are resistant to high-fat diet-induced insulin resistance despite reduced energy expenditure and ectopic lipid accumulation. *Endocrinology* 152(1):48-58.
28. Taschler U, Radner FP, Heier C, Schreiber R, Schweiger M, Schoiswohl G, Preiss-Landl K, Jaeger D, Reiter B, Koefeler HC, Wojciechowski J, Theussl C, Penninger JM, Lass A, Haemmerle G, Zechner R, & Zimmermann R (2011) Monoglyceride lipase deficiency in mice impairs lipolysis and attenuates diet-induced insulin resistance. *J Biol Chem* 286(20):17467-17477.
29. Perry RJ, Camporez JP, Kursawe R, Titchenell PM, Zhang D, Perry CJ, Jurczak MJ, Abudukadier A, Han MS, Zhang XM, Ruan HB, Yang X, Caprio S, Kaech SM, Sul HS, Birnbaum MJ, Davis RJ, Cline GW, Petersen KF, & Shulman GI (2015) Hepatic acetyl CoA links adipose tissue inflammation to hepatic insulin resistance and type 2 diabetes. *Cell* 160(4):745-758.
30. Amati F (2012) Revisiting the diacylglycerol-induced insulin resistance hypothesis. *Obes Rev* 13 Suppl 2:40-50.
31. Muoio DM (2010) Intramuscular triacylglycerol and insulin resistance: guilty as charged or wrongly accused? *Biochim Biophys Acta* 1801(3):281-288.
32. Muoio DM & Koves TR (2007) Lipid-induced metabolic dysfunction in skeletal muscle. *Novartis Found Symp* 286:24-38; discussion 38-46, 162-163, 196-203.
33. Zuurbier CJ, Hoek FJ, van Dijk J, Abeling NG, Meijers JC, Levels JH, de Jonge E, de Mol BA, & Van Wezel HB (2008) Perioperative hyperinsulinaemic normoglycaemic clamp causes hypolipidaemia after coronary artery surgery. *Br J Anaesth* 100(4):442-450.
34. Ljungqvist O (2010) Insulin resistance and outcomes in surgery. *J Clin Endocrinol Metab* 95(9):4217-4219.
35. Li L & Messina JL (2009) Acute insulin resistance following injury. *Trends Endocrinol Metab* 20(9):429-435.
36. Li L, Thompson LH, Zhao L, & Messina JL (2009) Tissue-specific difference in the molecular mechanisms for the development of acute insulin resistance after injury. *Endocrinology* 150(1):24-32.
37. Desborough JP (2000) The stress response to trauma and surgery. *Br J Anaesth* 85(1):109-117.
38. Butler SO, Btaiche IF, & Alaniz C (2005) Relationship between hyperglycemia and infection in critically ill patients. *Pharmacotherapy* 25(7):963-976.

39. Moore FD (1959) *Metabolic care of the surgical patient* (Saunders, Philadelphia,) p 1011 p.
40. Investigators N-SS, Finfer S, Chittock DR, Su SY, Blair D, Foster D, Dhingra V, Bellomo R, Cook D, Dodek P, Henderson WR, Hebert PC, Heritier S, Heyland DK, McArthur C, McDonald E, Mitchell I, Myburgh JA, Norton R, Potter J, Robinson BG, & Ronco JJ (2009) Intensive versus conventional glucose control in critically ill patients. *N Engl J Med* 360(13):1283-1297.
41. van den Berghe G, Wouters P, Weekers F, Verwaest C, Bruyninckx F, Schetz M, Vlasselaers D, Ferdinande P, Lauwers P, & Bouillon R (2001) Intensive insulin therapy in critically ill patients. *N Engl J Med* 345(19):1359-1367.
42. Wiener RS, Wiener DC, & Larson RJ (2008) Benefits and risks of tight glucose control in critically ill adults: a meta-analysis. *JAMA* 300(8):933-944.
43. Mesotten D & Van den Berghe G (2012) Glycemic targets and approaches to management of the patient with critical illness. *Curr Diab Rep* 12(1):101-107.
44. Finfer S, Heritier S, Committee NSM, & Committee SSE (2009) The NICE-SUGAR (Normoglycaemia in Intensive Care Evaluation and Survival Using Glucose Algorithm Regulation) Study: statistical analysis plan. *Crit Care Resusc* 11(1):46-57.
45. Van den Berghe G, Schetz M, Vlasselaers D, Hermans G, Wilmer A, Bouillon R, & Mesotten D (2009) Clinical review: Intensive insulin therapy in critically ill patients: NICE-SUGAR or Leuven blood glucose target? *J Clin Endocrinol Metab* 94(9):3163-3170.
46. Carvalho E, Kotani K, Peroni OD, & Kahn BB (2005) Adipose-specific overexpression of GLUT4 reverses insulin resistance and diabetes in mice lacking GLUT4 selectively in muscle. *Am J Physiol Endocrinol Metab* 289(4):E551-561.
47. Williams VL, Martin RE, Franklin JL, Hardy RW, & Messina JL (2012) Injury-induced insulin resistance in adipose tissue. *Biochem Biophys Res Commun* 421(3):442-448.
48. Wullschleger S, Loewith R, & Hall MN (2006) TOR signaling in growth and metabolism. *Cell* 124(3):471-484.
49. Laplante M & Sabatini DM (2009) An emerging role of mTOR in lipid biosynthesis. *Curr Biol* 19(22):R1046-1052.
50. Laplante M & Sabatini DM (2012) mTOR signaling in growth control and disease. *Cell* 149(2):274-293.
51. Sengupta S, Peterson TR, & Sabatini DM (2010) Regulation of the mTOR complex 1 pathway by nutrients, growth factors, and stress. *Mol Cell* 40(2):310-322.
52. Nojima H, Tokunaga C, Eguchi S, Oshiro N, Hidayat S, Yoshino K, Hara K, Tanaka N, Avruch J, & Yonezawa K (2003) The mammalian target of rapamycin (mTOR) partner, raptor, binds the mTOR substrates p70 S6 kinase and 4E-BP1 through their TOR signaling (TOS) motif. *J Biol Chem* 278(18):15461-15464.
53. Fang Y, Vilella-Bach M, Bachmann R, Flanigan A, & Chen J (2001) Phosphatidic acid-mediated mitogenic activation of mTOR signaling. *Science* 294(5548):1942-1945.
54. Foster DA (2007) Regulation of mTOR by phosphatidic acid? *Cancer Res* 67(1):1-4.
55. Harrington LS, Findlay GM, Gray A, Tolkacheva T, Wigfield S, Rebholz H, Barnett J, Leslie NR, Cheng S, Shepherd PR, Gout I, Downes CP, & Lamb RF (2004) The TSC1-2 tumor suppressor controls insulin-PI3K signaling via regulation of IRS proteins. *J Cell Biol* 166(2):213-223.
56. Laplante M & Sabatini DM (2009) mTOR signaling at a glance. *J Cell Sci* 122(Pt 20):3589-3594.
57. Jewell JL & Guan KL (2013) Nutrient signaling to mTOR and cell growth. *Trends Biochem Sci* 38(5):233-242.
58. Jaafar R, Zeiller C, Pirola L, Di Grazia A, Naro F, Vidal H, Lefai E, & Nemoz G (2011) Phospholipase D regulates myogenic differentiation through the activation of both mTORC1 and mTORC2 complexes. *J Biol Chem* 286(25):22609-22621.
59. Toschi A, Lee E, Xu L, Garcia A, Gadir N, & Foster DA (2009) Regulation of mTORC1 and mTORC2 complex assembly by phosphatidic acid: competition with rapamycin. *Mol Cell Biol* 29(6):1411-1420.

60. Sakamoto K & Holman GD (2008) Emerging role for AS160/TBC1D4 and TBC1D1 in the regulation of GLUT4 traffic. *Am J Physiol Endocrinol Metab* 295(1):E29-37.
61. Lansey MN, Walker NN, Hargett SR, Stevens JR, & Keller SR (2012) Deletion of Rab GAP AS160 modifies glucose uptake and GLUT4 translocation in primary skeletal muscles and adipocytes and impairs glucose homeostasis. *Am J Physiol Endocrinol Metab* 303(10):E1273-1286.
62. Jacinto E, Facchinetti V, Liu D, Soto N, Wei S, Jung SY, Huang Q, Qin J, & Su B (2006) SIN1/MIP1 maintains rictor-mTOR complex integrity and regulates Akt phosphorylation and substrate specificity. *Cell* 127(1):125-137.
63. Zhang C, Wendel AA, Keogh MR, Harris TE, Chen J, & Coleman RA (2012) Glycerolipid signals alter mTOR complex 2 (mTORC2) to diminish insulin signaling. *Proc Natl Acad Sci U S A* 109(5):1667-1672.
64. Ye L, Varamini B, Lamming DW, Sabatini DM, & Baur JA (2012) Rapamycin has a biphasic effect on insulin sensitivity in C2C12 myotubes due to sequential disruption of mTORC1 and mTORC2. *Front Genet* 3:177.
65. Sarbassov DD, Ali SM, Sengupta S, Sheen JH, Hsu PP, Bagley AF, Markhard AL, & Sabatini DM (2006) Prolonged rapamycin treatment inhibits mTORC2 assembly and Akt/PKB. *Mol Cell* 22(2):159-168.
66. Krebs M, Brunmair B, Brehm A, Artwohl M, Szendroedi J, Nowotny P, Roth E, Furnsinn C, Promintzer M, Anderwald C, Bischof M, & Roden M (2007) The Mammalian target of rapamycin pathway regulates nutrient-sensitive glucose uptake in man. *Diabetes* 56(6):1600-1607.
67. Johnston O, Rose CL, Webster AC, & Gill JS (2008) Sirolimus is associated with new-onset diabetes in kidney transplant recipients. *J Am Soc Nephrol* 19(7):1411-1418.
68. Pereira MJ, Palming J, Rizell M, Aureliano M, Carvalho E, Svensson MK, & Eriksson JW (2012) mTOR inhibition with rapamycin causes impaired insulin signalling and glucose uptake in human subcutaneous and omental adipocytes. *Mol Cell Endocrinol* 355(1):96-105.
69. Kumar A, Harris TE, Keller SR, Choi KM, Magnuson MA, & Lawrence JC, Jr. (2008) Muscle-specific deletion of rictor impairs insulin-stimulated glucose transport and enhances Basal glycogen synthase activity. *Mol Cell Biol* 28(1):61-70.
70. Wang L, Rhodes CJ, & Lawrence JC, Jr. (2006) Activation of mammalian target of rapamycin (mTOR) by insulin is associated with stimulation of 4EBP1 binding to dimeric mTOR complex 1. *J Biol Chem* 281(34):24293-24303.
71. Lin TA, Kong X, Saltiel AR, Blackshear PJ, & Lawrence JC, Jr. (1995) Control of PHAS-I by insulin in 3T3-L1 adipocytes. Synthesis, degradation, and phosphorylation by a rapamycin-sensitive and mitogen-activated protein kinase-independent pathway. *J Biol Chem* 270(31):18531-18538.
72. Pearce LR, Huang X, Boudeau J, Pawlowski R, Wullschleger S, Deak M, Ibrahim AF, Gourlay R, Magnuson MA, & Alessi DR (2007) Identification of Protor as a novel Rictor-binding component of mTOR complex-2. *Biochem J* 405(3):513-522.
73. Severgnini M, Sherman J, Sehgal A, Jayaprakash NK, Aubin J, Wang G, Zhang L, Peng CG, Yucius K, Butler J, & Fitzgerald K (2012) A rapid two-step method for isolation of functional primary mouse hepatocytes: cell characterization and asialoglycoprotein receptor based assay development. *Cytotechnology* 64(2):187-195.
74. Liu SC, Wang Q, Lienhard GE, & Keller SR (1999) Insulin receptor substrate 3 is not essential for growth or glucose homeostasis. *J Biol Chem* 274(25):18093-18099.
75. Murphy RC, James PF, McAnoy AM, Krank J, Duchoslav E, & Barkley RM (2007) Detection of the abundance of diacylglycerol and triacylglycerol molecular species in cells using neutral loss mass spectrometry. *Anal Biochem* 366(1):59-70.
76. Laplante M & Sabatini DM (2012) mTOR Signaling. *Cold Spring Harb Perspect Biol* 4(2).

77. Schweiger M, Schreiber R, Haemmerle G, Lass A, Fledelius C, Jacobsen P, Tornqvist H, Zechner R, & Zimmermann R (2006) Adipose triglyceride lipase and hormone-sensitive lipase are the major enzymes in adipose tissue triacylglycerol catabolism. *J Biol Chem* 281(52):40236-40241.
78. Kienesberger PC, Lee D, Pulinilkunnil T, Brenner DS, Cai L, Magnes C, Koefeler HC, Streith IE, Rechberger GN, Haemmerle G, Flier JS, Zechner R, Kim YB, & Kershaw EE (2009) Adipose triglyceride lipase deficiency causes tissue-specific changes in insulin signaling. *J Biol Chem* 284(44):30218-30229.
79. Ong KT, Mashek MT, Bu SY, & Mashek DG (2013) Hepatic ATGL knockdown uncouples glucose intolerance from liver TAG accumulation. *FASEB J* 27(1):313-321.
80. Lin TA & Lawrence JC, Jr. (1996) Control of the translational regulators PHAS-I and PHAS-II by insulin and cAMP in 3T3-L1 adipocytes. *J Biol Chem* 271(47):30199-30204.
81. Monfar M, Lemon KP, Grammer TC, Cheatham L, Chung J, Vlahos CJ, & Blenis J (1995) Activation of pp70/85 S6 kinases in interleukin-2-responsive lymphoid cells is mediated by phosphatidylinositol 3-kinase and inhibited by cyclic AMP. *Mol Cell Biol* 15(1):326-337.
82. Scott PH & Lawrence JC, Jr. (1998) Attenuation of mammalian target of rapamycin activity by increased cAMP in 3T3-L1 adipocytes. *J Biol Chem* 273(51):34496-34501.
83. Blancquaert S, Wang L, Paternot S, Coulonval K, Dumont JE, Harris TE, & Roger PP (2010) cAMP-dependent activation of mammalian target of rapamycin (mTOR) in thyroid cells. Implication in mitogenesis and activation of CDK4. *Mol Endocrinol* 24(7):1453-1468.
84. Mottillo EP, Bloch AE, Leff T, & Granneman JG (2012) Lipolytic products activate peroxisome proliferator-activated receptor (PPAR) alpha and delta in brown adipocytes to match fatty acid oxidation with supply. *J Biol Chem* 287(30):25038-25048.
85. Li LO, Klett EL, & Coleman RA (2010) Acyl-CoA synthesis, lipid metabolism and lipotoxicity. *Biochim Biophys Acta* 1801(3):246-251.
86. Samuel VT, Petersen KF, & Shulman GI (2010) Lipid-induced insulin resistance: unravelling the mechanism. *Lancet* 375(9733):2267-2277.
87. Wang S, Soni KG, Semache M, Casavant S, Fortier M, Pan L, & Mitchell GA (2008) Lipolysis and the integrated physiology of lipid energy metabolism. *Mol Genet Metab* 95(3):117-126.
88. Tozzo E, Kahn BB, Pilch PF, & Kandror KV (1996) Glut4 is targeted to specific vesicles in adipocytes of transgenic mice overexpressing Glut4 selectively in adipose tissue. *J Biol Chem* 271(18):10490-10494.
89. Nielsen TS, Jessen N, Jorgensen JO, Moller N, & Lund S (2014) Dissecting adipose tissue lipolysis: molecular regulation and implications for metabolic disease. *J Mol Endocrinol* 52(3):R199-R222.
90. Bochkov VN, Oskolkova OV, Birukov KG, Levonen AL, Binder CJ, & Stockl J (2010) Generation and biological activities of oxidized phospholipids. *Antioxid Redox Signal* 12(8):1009-1059.
91. Bournat JC & Brown CW (2010) Mitochondrial dysfunction in obesity. *Curr Opin Endocrinol Diabetes Obes* 17(5):446-452.
92. Greig FH, Kennedy S, & Spickett CM (2012) Physiological effects of oxidized phospholipids and their cellular signaling mechanisms in inflammation. *Free Radic Biol Med* 52(2):266-280.
93. Berliner JA, Leitinger N, & Tsimikas S (2009) The role of oxidized phospholipids in atherosclerosis. *J Lipid Res* 50 Suppl:S207-212.
94. Itani SI, Ruderman NB, Schmieder F, & Boden G (2002) Lipid-induced insulin resistance in human muscle is associated with changes in diacylglycerol, protein kinase C, and IkappaB-alpha. *Diabetes* 51(7):2005-2011.
95. Itani SI, Zhou Q, Pories WJ, MacDonald KG, & Dohm GL (2000) Involvement of protein kinase C in human skeletal muscle insulin resistance and obesity. *Diabetes* 49(8):1353-1358.
96. Yu C, Chen Y, Cline GW, Zhang D, Zong H, Wang Y, Bergeron R, Kim JK, Cushman SW, Cooney GJ, Atcheson B, White MF, Kraegen EW, & Shulman GI (2002) Mechanism by which

fatty acids inhibit insulin activation of insulin receptor substrate-1 (IRS-1)-associated phosphatidylinositol 3-kinase activity in muscle. *J Biol Chem* 277(52):50230-50236.

97. Sun Z & Lazar MA (2013) Dissociating fatty liver and diabetes. *Trends Endocrinol Metab* 24(1):4-12.
98. Goodpaster BH & Kelley DE (2002) Skeletal muscle triglyceride: marker or mediator of obesity-induced insulin resistance in type 2 diabetes mellitus? *Curr Diab Rep* 2(3):216-222.
99. Pan DA, Lillioja S, Kriketos AD, Milner MR, Baur LA, Bogardus C, Jenkins AB, & Storlien LH (1997) Skeletal muscle triglyceride levels are inversely related to insulin action. *Diabetes* 46(6):983-988.
100. Goodpaster BH, He J, Watkins S, & Kelley DE (2001) Skeletal muscle lipid content and insulin resistance: evidence for a paradox in endurance-trained athletes. *J Clin Endocrinol Metab* 86(12):5755-5761.
101. Yore MM, Syed I, Moraes-Vieira PM, Zhang T, Herman MA, Homan EA, Patel RT, Lee J, Chen S, Peroni OD, Dhaneshwar AS, Hammarstedt A, Smith U, McGraw TE, Saghatelian A, & Kahn BB (2014) Discovery of a class of endogenous mammalian lipids with anti-diabetic and anti-inflammatory effects. *Cell* 159(2):318-332.
102. Fridlyand LE & Philipson LH (2006) Reactive species, cellular repair and risk factors in the onset of type 2 diabetes mellitus: review and hypothesis. *Curr Diabetes Rev* 2(2):241-259.
103. Murdolo G, Piroddi M, Luchetti F, Tortoioli C, Canonico B, Zerbinati C, Galli F, & Iuliano L (2013) Oxidative stress and lipid peroxidation by-products at the crossroad between adipose organ dysregulation and obesity-linked insulin resistance. *Biochimie* 95(3):585-594.
104. Houstis N, Rosen ED, & Lander ES (2006) Reactive oxygen species have a causal role in multiple forms of insulin resistance. *Nature* 440(7086):944-948.
105. Gao CL, Zhu C, Zhao YP, Chen XH, Ji CB, Zhang CM, Zhu JG, Xia ZK, Tong ML, & Guo XR (2010) Mitochondrial dysfunction is induced by high levels of glucose and free fatty acids in 3T3-L1 adipocytes. *Mol Cell Endocrinol* 320(1-2):25-33.
106. Furukawa S, Fujita T, Shimabukuro M, Iwaki M, Yamada Y, Nakajima Y, Nakayama O, Makishima M, Matsuda M, & Shimomura I (2004) Increased oxidative stress in obesity and its impact on metabolic syndrome. *J Clin Invest* 114(12):1752-1761.
107. Veverka V, Crabbe T, Bird I, Lennie G, Muskett FW, Taylor RJ, & Carr MD (2008) Structural characterization of the interaction of mTOR with phosphatidic acid and a novel class of inhibitor: compelling evidence for a central role of the FRB domain in small molecule-mediated regulation of mTOR. *Oncogene* 27(5):585-595.
108. Ogden CL, Carroll MD, Kit BK, & Flegal KM (2012) Prevalence of obesity in the United States, 2009-2010. *NCHS Data Brief* (82):1-8.
109. Muoio DM & Newgard CB (2008) Mechanisms of disease: molecular and metabolic mechanisms of insulin resistance and beta-cell failure in type 2 diabetes. *Nat Rev Mol Cell Biol* 9(3):193-205.
110. Delarue J & Magnan C (2007) Free fatty acids and insulin resistance. *Curr Opin Clin Nutr Metab Care* 10(2):142-148.
111. Lee YH & Pratley RE (2005) The evolving role of inflammation in obesity and the metabolic syndrome. *Curr Diab Rep* 5(1):70-75.
112. Engeli S & Sharma AM (2000) Role of adipose tissue for cardiovascular-renal regulation in health and disease. *Horm Metab Res* 32(11-12):485-499.
113. Hall JE, Hildebrandt DA, & Kuo J (2001) Obesity hypertension: role of leptin and sympathetic nervous system. *Am J Hypertens* 14(6 Pt 2):103S-115S.
114. Watson AD, Leitinger N, Navab M, Faull KF, Horkko S, Witztum JL, Palinski W, Schwenke D, Salomon RG, Sha W, Subbanagounder G, Fogelman AM, & Berliner JA (1997) Structural identification by mass spectrometry of oxidized phospholipids in minimally oxidized low density lipoprotein that induce monocyte/endothelial interactions and evidence for their presence in vivo. *J Biol Chem* 272(21):13597-13607.

115. Ma Y, Wang P, Kuebler JF, Chaudry IH, & Messina JL (2003) Hemorrhage induces the rapid development of hepatic insulin resistance. *Am J Physiol Gastrointest Liver Physiol* 284(1):G107-115.
116. Corrick RM, Li L, Frank SJ, & Messina JL (2013) Hepatic growth hormone resistance after acute injury. *Endocrinology* 154(4):1577-1588.